Tellus Merge-2022 Airborne Geophysical Technical Report

(Operations, Logistics and Data Merging)

Geological Survey Ireland is a division of the Department of Communications, Climate Action & Environment.

Geological Survey
Suirbhéireacht Gheolaíochta
Ireland | Éireann

Document Information

Project title: Tellus Merge-2022 (A6, A8, A9 Blocks) Airborne Geophysics Technical Report Current Document version V3
Date 10 March 2022

Prepared By	Date	Comment
M.D. Ture	10/03/2022	V3

Reviewed By	Date	Comment
M.R. Muller	21/02/2022, 02/03/2022	Reviews of V1, V2
J.A. Hodgson	23/02/2022	Review of V1

Approved By	Date	Comment

Version History

Ver. No.	Ver. Date	Comment	Revised By
V1	17/02/2022		M.D. Ture
V2	25/02/2022	Following M.R. Muller and J.A. Hodgson review	M.D. Ture
V3	10/03/2022	Following M.R. Muller review	M.D. Ture

The Tellus Project

Tellus is a national programme to gather geochemical and geophysical data across the island of Ireland. The survey examines the chemical and physical properties of our soils, rocks and waters to inform the management of Ireland's environment and natural resources. The project is managed by Geological Survey Ireland and is funded by the Department of Environment, Climate and Communications (DECC).

For more information on the Tellus Project please visit www.gsi.ie/tellus.

Executive Summary

Tellus is a national airborne geophysics mapping programme of Ireland and follows on from the Tellus Survey of Northern Ireland in 2005-2006, with the first survey carried out in Ireland in 2011. Since then annual survey blocks have generally progressed southwards through the country. The latest phase of the Tellus programme collected airborne data over two new blocks (A8 and A9) in South Ireland (Counties of Tipperary, Kilkenny, Laois and Waterford) & County Cork and are referred to as blocks A8 and A9 respectively. Surveying was carried out between 20 September 2020 and 15 July 2021 (A8) and between 25 July 2021 and 21 September 2021 (A9) by Sander Geophysics Ltd (SGL). Previous airborne geophysical surveys were carried out across Northern Ireland (Tellus) in 2005 and 2006 (Beamish *et. al*, 2006), parts of counties Cavan and Monaghan in the ROI (Kurimo, 2006), counties Donegal, Leitrim, Sligo, Cavan, Monaghan and Louth as part of the EU INTERREG IVA-funded Tellus Border Project (Hodgson and Ture, 2012), across counties Roscommon, Longford and Westmeath as part of the Tellus North Midlands project (Hodgson and Ture, 2015), across parts of counties Meath, Dublin, Kildare, Offaly, Laois and Wicklow (Block A1) in the east of the country in 2015 (Hodgson and Ture, 2016) and across County Galway (Block A2) in 2016 (Hodgson and Ture, 2017) and across counties Mayo and Donegal (Blocks A3 and A4) in 2017 (Hodgson and Ture, 2018), across county Limerick and west Cork (Blocks A5 and A6) in 2018-2019 (Hodgson, Ture and Muller, 2019) and across counties Wexford, Wicklow, Kildare and Carlow (Block A7, SE Ireland) in 2019. The latest phases of airborne surveying, A8 and A9 blocks were flown with the same aircraft based at Waterford Airport. All surveys measured magnetic field, electrical conductivity and gamma-ray spectrometer data (primarily potassium, thorium and uranium).

This report summarizes the main operations from the latest A8 and A9 surveys and discusses the processing of the acquired data and its merging with pre-existing datasets to produce seamless merged geophysical datasets. The A6 Block (west Cork) has a small overlap with A9 and is included in the merging of the current data. It is anticipated, however, that a better constrained merge of A6 will be possible after completion of subsequent survey blocks, which will provide more substantial overlap with A6.

The following data SGL data delivery numbers have provided the data for Blocks A6, A8 and A9 (respectively) for the merge; for magnetics: DLV2160, DLV2420, DLV2554; for radiometrics DLV2161, DLV2419, DLV2433; for electromagnetics: DLV2159, DLV2421, DLV2439.

Acknowledgements

During the operation of the survey, Emma Scanlon and Margaret Browne at GSI, along with the public relations company RPS, helped with the successful undertaking of the outreach Programme. The crew of SGL are thanked for their hard work throughout the duration of the survey.

Contents

Figures

Tables

1. Tellus Geophysical Surveys

1.1 Overview of Tellus Project and previous surveys

The Tellus survey Blocks A8 and A9 over the south of Ireland follow on from previous airborne surveys carried out under the Tellus Programme. These surveys include the original Tellus survey of Northern Ireland (2005-2006) and the EU INTERREG IVA-funded cross border survey of the border region of Ireland (2011-2012), the Tellus North Midlands survey (2014-2015) along with the survey of Block A1 (2015) in the east of the country and a survey of county Waterford (2016) in the south of the country and Block A2 over county Galway (2016), and across counties Mayo and Donegal (Blocks A3 and A4) in 2017, and across County Limerick and West Cork (Blocks A5 and A6 respectively) in 2018-2019 and A7 block over counties of Wicklow, Wexford, Kildare and Carlow in 2019 in the SE of Ireland. All airborne surveys comprised the collection of low-altitude magnetic, gamma-ray spectrometry and electromagnetic data. However, for the North Midlands survey, Time-Domain Electromagnetic (TEM) data were collected in contrast to Frequency-domain EM (FEM) data which were collected for the other surveys. Under the latest phase of the Tellus survey, airborne data were collected over Blocks A8 and A9, using the same aircraft and based at Waterford Airport, which is located close to the survey area. Following the completion of these latest phases (A8 and A9), approximately 80% of Republic of Ireland has now been surveyed, excluding Dublin City.

2. A8 and A9 Survey Operations & Specifications

The current survey areas, Blocks A8 and A9, are shown in Figures 1 & 2. Block A8 covers the majority of Counties Tipperary, Kilkenny, Laois and Waterford. The A9 block was flown over county Cork. Topography and land-use in the A8 and A9 areas are a mix of low-lying undulating grass farmlands and ranges of mountainous topography, such as Knockmealdown, Galty and Comeragh. There are also isolated mountains such Borrinoe, Kildoff, Devilsbit, Lyre and Wolftrap. A9 block includes Rahan, Moyanass and Rathcormack Mountains in the central part. The highest point in County Kilkenny is Lyre Mountain at 650 m and this lies just off the south eastern boundary of Block A9. A number of significant rivers (Nore, Barrow and Suir) flow through the region.

The A8 survey area was designed to allow an overlap with the Tellus A1, A5, A7, WFD and A9 blocks, while A9 was designed to have overlap with A8, A5 and A6 blocks, which would assist the merging of the data. The surveys were also designed within the context of a national survey and to complete more than 80% of this national survey by the end of 2021. The survey blocks discussed in this report are outlined in Figure 2.

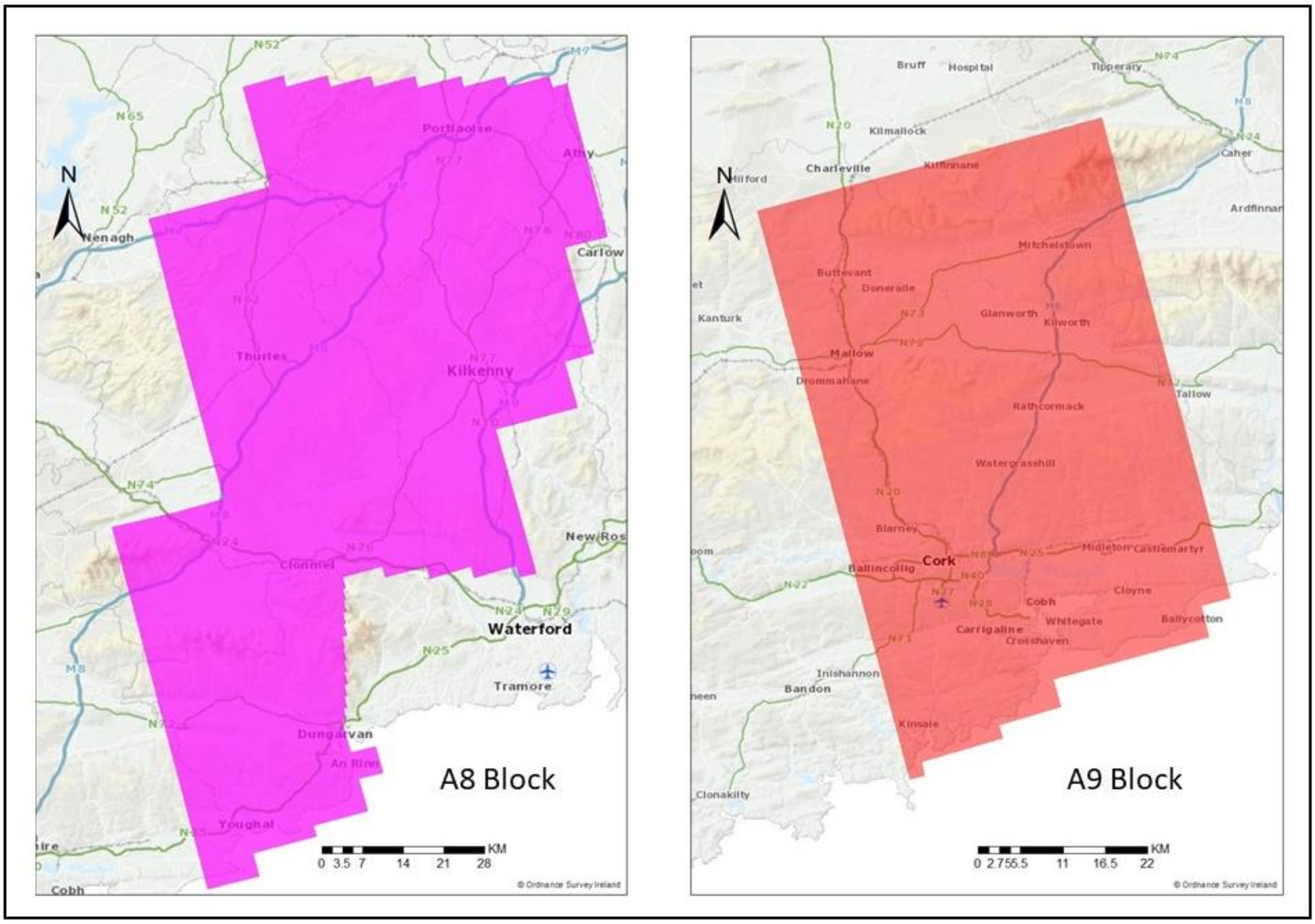

Figure 1: Tellus A8 block (left) and A9 block (right) survey areas over southern Ireland.

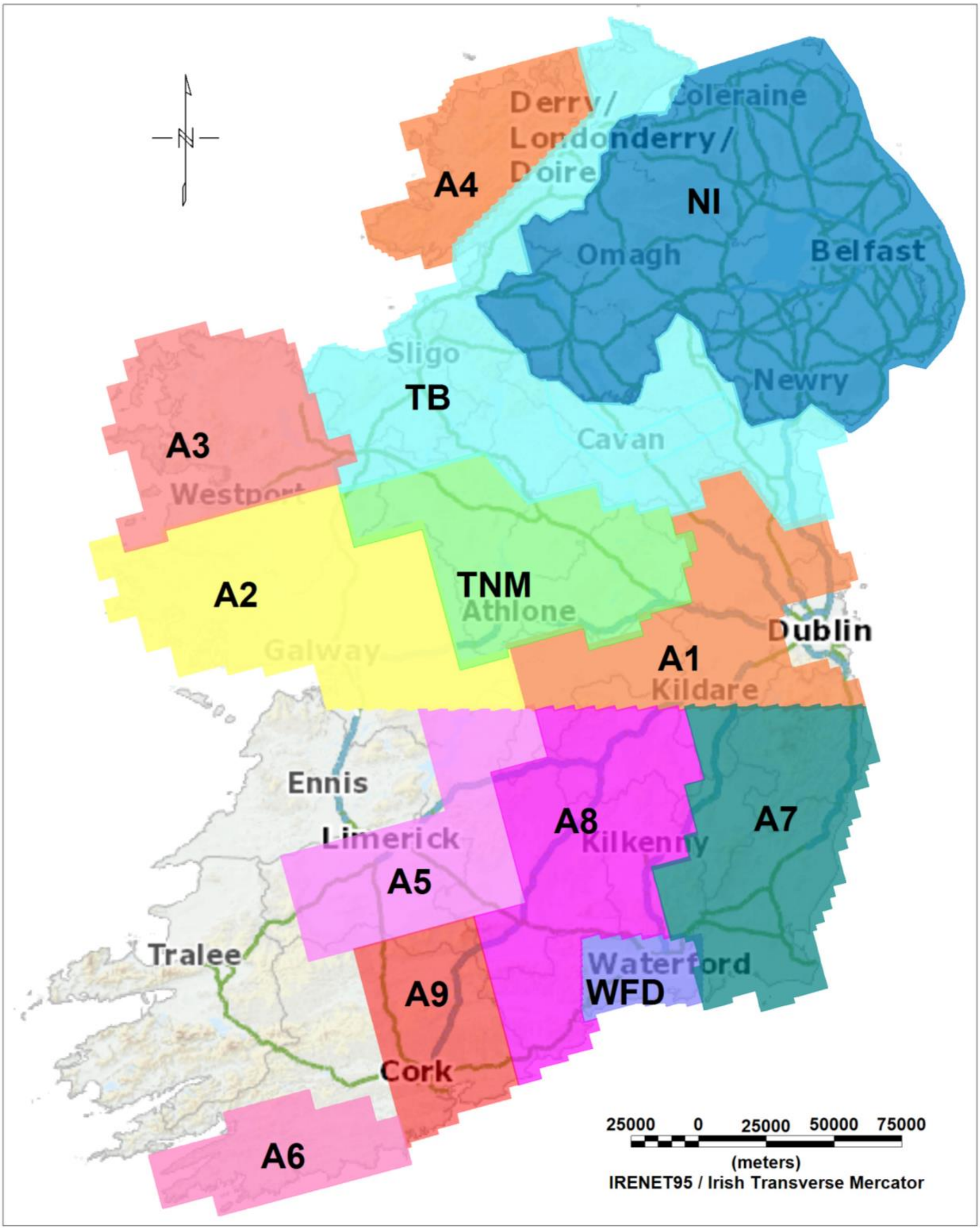

Figure 2: Tellus survey blocks 2005 – 2021.

Table 1: Tellus Survey Blocks showing year of survey and coverage area. The areas include overlap zones and coastal areas.

BLOCK	SURVEY YEAR	BLOCK AREA (km^2)
NI	2005/2006	16178
CAV	2006	1054
TB	2006, 2011-2012	10773
TNM	2014	5979
A1	2015	6015
A2	2016	7819
WFD	2016	1216
A3	2017	4992
A4	2017	3459
A5	2018	4638
A6	2018	2698
A7	2019	6476
A8	2020	6896
A9	2021	3288
Total airborne covered area		81,481
Total airborne covered area (ROI)		65,303
Total excl. overlap and coastal area (ROI)		**56,496**
Percent ROI (onshore) excl. Dublin		80.3%

2.1 Flight characteristics and survey pattern

The flight pattern is described in Table 2 below.

Table 2: Flight Pattern.

Traverse Line Spacing	200 m
Tie Line Spacing	2000 m
Traverse Line Heading	165/ 345^0
Tie-Line Heading	75/ 255^0
Flying Height (rural / urban)	60/ 240 m subject to pilot's discretion
Projection / Datum	Irish Transverse Mercator

A repeat test calibration line was established close to the town of Bundoran, Co. Donegal in the northwest of Ireland. The same test line was flown during the Tellus Border, North Midlands and A1, A2, A3, A4, A5 and A6 Surveys, allowing comparisons to be made between surveys. The test line is 6 km in length and was flown at six different elevations during each run. The line ran from off-shore to on-shore and was selected based on variable bedrock and superficial geological aspects, and is discussed further in Section 3.10.

From 2019 (Blocks A7, A8, A9) onward the Tellus project used a new test calibration line that was established close to the village of Kill, Co. Waterford in the south of Ireland, about 20 km to SW of Waterford city (see Figure 6). The test line is located between 646290 m E & 597625 m N and 644865 m E & 602937 m N in the ITM coordinate system. The Test line is 5.5 km long (with 4.5 km on land and 1 km over the sea).

2.2 Flight permits

The contractor (Sander Geophysics Ltd.) received the required Irish Aviation Authority (IAA) flight permits for its aircraft C-GSGF to conduct a low-level survey in Ireland.

2.3 Geographic projection

Final data were referenced to the Irish Transverse Mercator as defined in Table 3.

Table 3: Irish Transverse Mercator Geographic Projection.

IRISH TRANSVERSE MERCATOR	
Reference Ellipsoid:	GRS80
Central Meridian	08° 00’ 00” West
Vertical Datum:	Malin Head
Map Projection:	Transverse Mercator (Gauss Conformal)
True origin:	53° 30’ 00” North, 08° 00’ 00” West
False origin:	600 km west, 750 km south of true origin
Scale factor on Central Meridian:	0.999820

2.4 Re-flight conditions

Data were received from the contractor on a weekly basis for quality assessment. The following re-flight conditions were enforced during the survey:

- Where flight line deviation for traverse-lines is greater than 45 m from the planned line over a distance of 2.5 km or more, or greater than 90m from the planned line over any distance (except where ground conditions dictate otherwise, for example to avoid radio-masts etc.).
- Where flight line deviation for tie-lines is greater than 100 m from the planned line over a distance of 2.5 km or more, or any deviation greater than 200 m from the planned line over any distance.
- Where terrain clearance exceeds +/- 20 metres from the nominal survey height for more than 5 continuous kilometres or 40 m of nominal survey height at any time on any line, unless local topography makes this unavoidable.
- Where the nominal survey flying speed (60 m/s) is exceeded by more than 30% (78 m/s) for more than 5 continuous kilometres.
- Where the noise envelope of the magnetic records exceeds 0.1 nT as determined by the normalised fourth difference.
- If, during data acquisition, magnetic variations recorded at the local base magnetometer exceed 12 nT over any 3-minute chord or exceed 2 nT over any 30 second chord, on flight lines or tie lines. The base magnetometer must be fully operational during all on-line data collection.
- Where the average line gamma spectra for any line appears anomalous by comparison with previously acquired data then the data of that line will be investigated in detail and re-flown if necessary.
- If the calibration of the EM system deviates significantly from the norm.
- If both primary and secondary GPS base stations fail to record for 30 minutes or more, simultaneously.
- If both primary and secondary magnetic base stations fail to record for 30 minutes or more, simultaneously.

These conditions may be exceeded without re-flight where such constraints would breach air safety regulations, or in the opinion of the pilot, put the aircraft and crew at risk. All such exceptions were logged and a log of all flights can be found in the technical report produced by SGL (2016, 2017, 2019 and 2021). Data generally met the required specifications, although some altitude deviations were encountered; these were often related to client enforced high fly zones due to urban areas, stud farms, radio masts and pilot safety requirements.

2.5 Survey equipment and aircraft systems

2.5.1 Survey Aircraft

The contractor, Sander Geophysics Ltd., used a De Havilland DHC-6 twin Otter (registration number C-GSGF) for all survey work. The same aircraft was used in the Tellus survey of Northern Ireland (2005-6), under the registration OH-KOG. During the Northern Ireland survey, it was operated by JAC (Joint Airborne-geoscience Capability), which was a partnership between the Geological Survey of Finland and the British Geological Survey. The aircraft was also used under its current registration for the Tellus Border Survey (2011-2012), A1 and A2 Surveys (2015 & 2016), A3 and A4 surveys (2017), A5 and A6 surveys (2018-2019), A7 survey (2019), A8 survey (2020-2021) and A9 (2021). This aircraft is an all metal, fixed-wing, twin-engine, short take-off and landing aircraft (Figure 3). The aircraft can be flown at speeds from 80 to 160 knots (41 to 82 m/s). The Twin Otter is equipped with airborne magnetic, radiometric and frequency-domain electromagnetic (FEM) systems as outlined by Hautaniemi *et al*., 2005. The aircraft houses two magnetometers, one attached to a rear boom and one in the left wing tip pod. The four frequency EM transmitter was housed in the right wing tip pod and the receiver in the left wing tip pod. The Gamma Ray spectrometer crystal packs were housed in the rear of the aircraft (Figure 4) and also in the undercarriage to accommodate additional crystal packs.

The NavDAS system developed by SGL was used for airborne navigation and data acquisition. The system displays all incoming data on a flat panel screen for real-time monitoring.

Figure 3: Survey Aircraft – De Havilland Twin Otter, C-GSGF.

2.5.2 Geophysical Instrumentation

Table 4 below outlines the survey equipment used by SGL during the project. Further detail of the instrumentation is given by SGL (2021).

Table 4: Survey Equipment.

Survey Method	Equipment used
Magnetometer	Aircraft: 2 x Geometrics G-822A, optically pumped Caesium split beam sensors, tail stinger and wing tip, sampling rate:10 Hz Base station: 2 x Geometrics G-822A SGComp, post-flight compensation
EM system	SGFEM: Four frequency (0.9, 3, 12 and 25 kHz), sampling 10 Hz. Wingtip coils
Gamma-ray spectrometer	Radiation Solution RS-501 gamma-ray spectrometer 1024-channels, self-calibrating, 67.2 litres downward, 12.6 litres upward looking, pressure and temperature sensors, sampling rate 1 Hz.
Altimeter	Collins radar altimeter (AL-101), sampling 10 Hz SGLas-P Riegl laser rangefinder altimeter LD90-3300VHS-FLP, 20 Hz sampling rate Honeywell Barometric Pressure sensor, 10 Hz sampling rate Omega RTD-805 Outside air temperature probe
GPS	SGRef system, DGPS receiver (10 Hz) NovAtel Millenium 12 channel dual frequency
Video	SGDIS – Digital imaging system (avi format)
Data location system	Post-process DGPS based on NovAtel OEM-V receivers in aircraft and at base.
Data transfer medium	Solid state hard drives and FTP

Magnetometers

Geometrics G-822A and optically pumped Caesium-split beam magnetometers, were used for both ground and aircraft sensors respectively. The Caesium magnetometers were housed on the left wing pod and within a rear tail stinger. The two base station magnetometers were located close to the field base. All magnetometers had a sensitivity of 0.005 nT and range of 20,000 to 100,000 nT with a sensor noise less than 0.02 nT. Measurements were delivered at 10 Hz intervals.

Spectrometers

The Gamma Ray spectrometer system used was Radiation Solutions RS-501 with Crystal Detector packs RS5557, RS5558, RS5444, RS5632, with 1024 channels. The system used 16 x 4.2 litre downward looking and 3 x 4.2 litre upwards looking NaI crystals of total volume of 67.2 and 12.6 litres respectively. Data were collected at a sampling rate of 1 second in 1024 channel spectral mode. The system was calibrated at the Geological Survey of Canada's test range at Breckenridge, Quebec, along with a ground calibration pad test in Ottawa, Canada before departure to Ireland. Hand sample checks were run on the gamma ray spectrometer before or after each day's flying to check spectral stability and system sensitivity. Relative count rates were measured to achieve background rates that were within two standard deviations of the average sample checks for the survey.

Frequency-domain electromagnetic system

The SGFEM system used four frequencies, 912, 3005, 11962 and 24510 Hz with a transmitter-receiver coil separation of 21.4 m. The transmitter-receiver coil pairs were mounted in a vertical-coplanar orientation which helped reduce noise by minimising coupling with the wingtip surface. A 50/60 Hz power line monitor was also employed to help identify cultural interference related to power lines. Data was sampled at 40 Hz and later decimated to 10 Hz by the contractor during processing of the data.

Figure 4: Radiation Solutions spectrometer housed in the aircraft.

2.5.3 Altimeter system

Four types of altimeter were employed on the aircraft. These were:

- SGLas-P – Riegl LD90-3300VHS-FLP Laser Rangefinder: This laser altimeter has a range of 338 m and a resolution of 0.01 m with an accuracy of 5 cm and a sample rate of 20 Hz data rate later decimated to 10 Hz.
- Collins AL-101 Radar Altimeter: This radar altimeter has a resolution of 0.5 m, an accuracy of 5%, a range of 0 to 408 m and was sampled at 10 Hz.
- Honeywell Barometric Pressure Sensor: Measures static pressure to an accuracy of ± 4 m with a resolution of up to 2 m over range of 0 to 9,144 m above sea level. Barometric pressure is sampled at 10 Hz.
- Omega RTD-805 Outside Air-temperature probe: Sampled at 10Hz with a resolution of 0.1 ^{0}C with a range of +/- 100 ^{0}C and an accuracy of ± 0.2^{0}C.

2.5.4 Magnetic Base Station

Two reference stations were installed for A8 and A9 surveys. GND1 was located at the airport south of the CHC hangar behind the fuel farm and GND2 was located at a farm just north of Dunmore East, County Wexford.

The Geometrics G-822A magnetometers were used to measure the daily diurnal variation during the survey. The co-ordinates for the base stations are shown in table 5 below:

Table 5: Co-ordinates of magnetic base stations used during the A8 and A9 surveys.

Station	Easting	Northing	Projection	Elevation
GND1	W07°04'47.2”	N52°11'23.5''	WGS84	83.7 m
GND2	W07°00'39.5''	N52°09'21.0''	WGS84	107.6 m
GND1	662919.94	604622.03	ITM	83.7 m
GND2	667680.34	600901.64	ITM	107.6m

3. Start-up Calibrations & Mobilisation

3.1 Calibrations Introduction

The airborne geophysical equipment system calibrations and tests prior to mobilization were carried out in Ottawa, Canada, as well as at the Geological Survey of Canada's Breckenridge Calibration Range in Quebec; further calibrations were also conducted on site in Ireland. The details of all these tests were reported by SGL and are also outlined in the SGL Technical Report TR-888-000 (2021). The main calibrations, which were carried out as part of the survey, are summarized below.

3.2 Magnetic Compensation

Compensation calibrations determine the magnetic influence of aircraft and its maneuvers. During the compensation calibration flight, the aircraft performs sets of three pitches (+/-5º), rolls (+/-10º), and yaws (+/-5º), while flying in the four flight line directions at high altitude over a magnetically quiet area. The coefficients calculated from the calibration are applied to the acquired magnetometer data to measure the effectiveness of the compensation system in mitigating the aircraft's magnetic interference.

The total compensated signal noise resulting from the twelve maneuvers, referred to as the Figure of Merit (FOM), is calculated from the maximum peak-to-peak value resulting from each maneuver. A compensation calibration was performed on June 9 2020 for the tail magnetometer before the aircraft left Ottawa and recorded a Figure of Merit (FOM) value of 0.73 nT, within the required specifications. A compensation test flight was also performed in Ireland on 9 October 2020. The FOM for this test flight was 1.07 nT, within specification.

3.3 Heading Error Determination

A heading test was performed over the Morewood test site in Ontario, Canada on June 16, 2020 before the aircraft ferried to Ireland. The heading test flight lines were pre-planned, and reference ground magnetic data were obtained through the use of the SGL head office reference station. The test determined an average north-south heading error of 0.83 nT and an average east-west heading error of 1.45 nT for the tail magnetometer. The heading error remains consistent through the duration of the survey, and is fully corrected in the normal airborne magnetic data during processing.

3.4 Lag and Parallax Test

The lag in the magnetic data is a function of two components, a static lag due to signal processing and a speed-dependent dynamic lag due to the physical offset of the magnetometer and the GPS antenna. Both elements of the lag are well-known. The static lag is known to be 0.244 s from the filters applied during signal processing. The dynamic lag is equal to the offset of the GPS sensor (located on the aircraft tail for this survey) to the tail magnetometer as measured along the long axis of the aircraft, known to be 4.27 m, divided by the flying speed. For a speed of 60 m/s the dynamic tail magnetometer lag will average 0.071 s, for a total lag of 0.32 s.

3.5 Radiometric Calibrations

The stripping ratios for the gamma-ray spectrometer were determined on July 7-8, 2020 before the aircraft departed Ottawa. The Geological Survey of Canada (GSC) calibration pads, which are stored at the SGL hangar in Ottawa, were used. The tests were performed with the detectors installed in survey configuration on board the aircraft. Each detector was tested separately and the test results were averaged to create stripping ratios for this system. Full details of these tests were reported by SGL, are contained in SGL technical Report 2021 and summarized in Table 5. Calibrations are carried out based on guidelines set out in IAEA (2003) and Grasty and Minty (1995).

Table 6: **Spectrometer Processing Parameters for A8 and A9 blocks.**

Spectrometer Processing Parameters – Spectrometer Radiation Solutions Model RS-501 NaI (Tl) crystals 67.2 L, Down, 12.6 L Up. At 60 m survey altitude.		
Window	**Cosmic Stripping Ratio (b)**	**Aircraft Background (a)**
Total	1.2728	10.0000
Potassium	0.0650	19.2299
Uranium	0.0420	0.0000
Thorium	0.0491	0.0000
Upward	*0.0072*	*0.0000*
Radon Correction	**Radon Ratio (a)**	**(b)**
Total (Ir)	*15.4608*	*0.0000*
Potassium	*0.7635*	*0.0000*
Thorium(Tr)	*0.0707*	*0.0000*
Upward Uranium(Ur)	*0.2100*	*0.0000*
Ground component	***a1***	***a2***
Up (ug)	*0.032891*	*0.024257*
Stripping Ratios	**Contribution on the ground**	**Effective height adjustment**
α	*0.2782*	*0.00049*
β	*0.4183*	*0.00065*
γ	*0.7820*	*0.00069*
a	*0.0453*	*0*
b	*0.0000*	*0*
g	*0.0032*	0
Attenuation Coefficients		
Total	-0.006849	
Potassium	*-0.007700*	
Uranium	*-0.007337*	
Thorium	*-0.006036*	
Sensitivities at 60m		
Total Count		
Potassium	*228.93 cps/%*	
Uranium	*23.79 cps/eU ppm*	
Thorium	*12.31 cps/eTh ppm*	

3.6 EM System Orthogonality

Prior to each flight, the phase shift between the in-phase and quadrature parts of the EM response is verified and adjusted if required. For each frequency, two pulses of constant amplitude are artificially generated, the first being perfectly in-phase with the primary field, and the second being phase shifted by 90 degrees. Therefore, when the phase orthogonality is properly adjusted, no quadrature response should be observed during the first pulse, and vice versa during the second. This test is usually performed above 300 m flight-height to avoid any EM response from the ground and to minimize cultural interference. The compensation of the primary field is verified, enabling EM data to be recorded with reference to an arbitrary zero-level low enough to ensure that the full range of the receiving device can be utilized. This ensures the system is functioning properly. The orthogonality check is also performed following each production flight, while ferrying back to the base.

3.7 EM Over-Seawater Calibration

The frequency domain electromagnetic system was calibrated following procedures described by Hautaniemi *et al.* (2005). Starting from the Tellus Northern Ireland survey in 2005 and up to the A5 & A6 survey blocks in 2018-2019, a test site was chosen over Donegal Bay, in an area where water conductivity and temperature have been measured several times over the years, at every meter from surface to sea floor, by the Irish Marine Institute. The water depth reaches over 60 m, ensuring that the bottom sediments do not contribute to the EM response. Conductivity data from two different stations taken from three different years were analysed, showing conductivity profiles to be essentially consistent at the two stations, and therefore data can be considered constant between the stations. The calibration line location (in red) and the two marine sampling stations (CE10003_056 and CE10003_057) are shown in Figure 5.

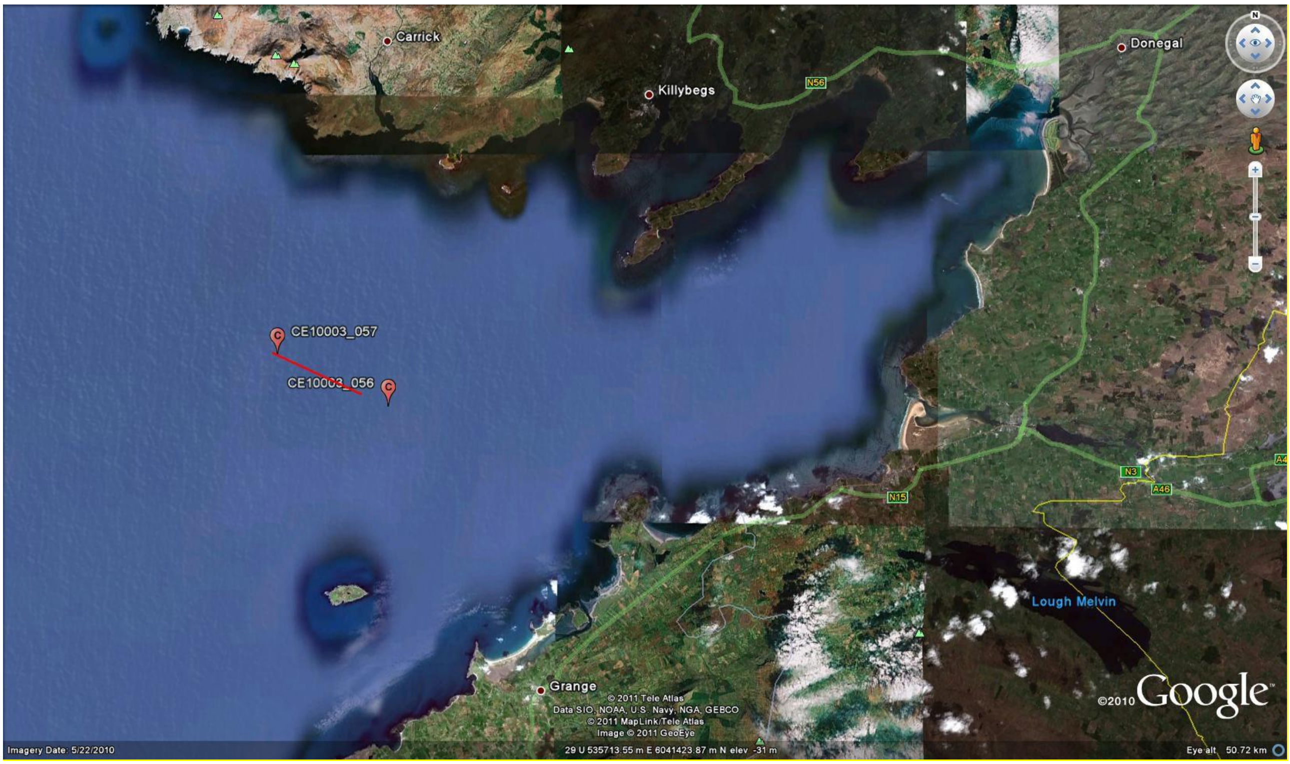

Figure 5: Location of overwater calibration line Over Donegal bay and marine sampling locations (2005-2018).

However, from 2019 (Block A7) onward the Tellus project used a new test site just south of Waterford (see Figure 6). Sea-surface salinity at the Waterford site, as provided by the Irish Marine Atlas, is within 0.1 g/l of the Donegal site (as measured in April, 2017), hence this new test site will have very similar resistivity and thermal characteristics to the Donegal Bay location outlined above. The Waterford test line includes an on-land portion to replace the "Bundoran" test line, as well as an over-sea-water portion for the EM calibration test. The central test line is simply extended over sea water and flown at multiple altitudes. The land and shallow portions of the test line are omitted when tabulating the calibration test results. The yellow box in Figure 6 outlines the data used in the over sea water test portion. The skin depths of all four frequencies are less than half the water depth so the sea-floor bottom has no impact and the homogenous half space model is valid. The water depth in the seawater test portion is greater than 22.5 m, for which a typical sea-floor bottom resistivity of 1.0 ohm-m would make less than 0.1% difference in the low-frequency in-phase amplitude, relative to deeper water.

Surface water temperature measured on the same day the calibration flight took place (14.209 ºC, measured at buoy M5 located approximately 65 km south east of the Waterford test line (51.6900ºN, 06.7040ºW) on October 11, 2020 as published by the Irish Marine Institute) enabled the estimation of the water conductivity close to surface ([0.089 S/m ºC * 14.209 ºC] + 2.915 S/m = 4.179 S/m). Based on the average conductivity decrease with depth observed over the three years in Donegal Bay, it was possible to estimate the water conductivity at a depth of 30m ([-0.0025 S/m^2 * 30 m] + 4.179 S/m = 4.105 S/m), and the average conductivity between the surface and a depth of 30 m at the calibration site (4.142 S/m). Slight changes in conductivity below 30 m are negligible. This conductivity was used to create a single layer model (half-space), which was employed to calculate the EM response for each component of each frequency, for the range of altitudes covered during the calibration flight. The calculation was performed with the software Airbeo, developed by AMIRA.

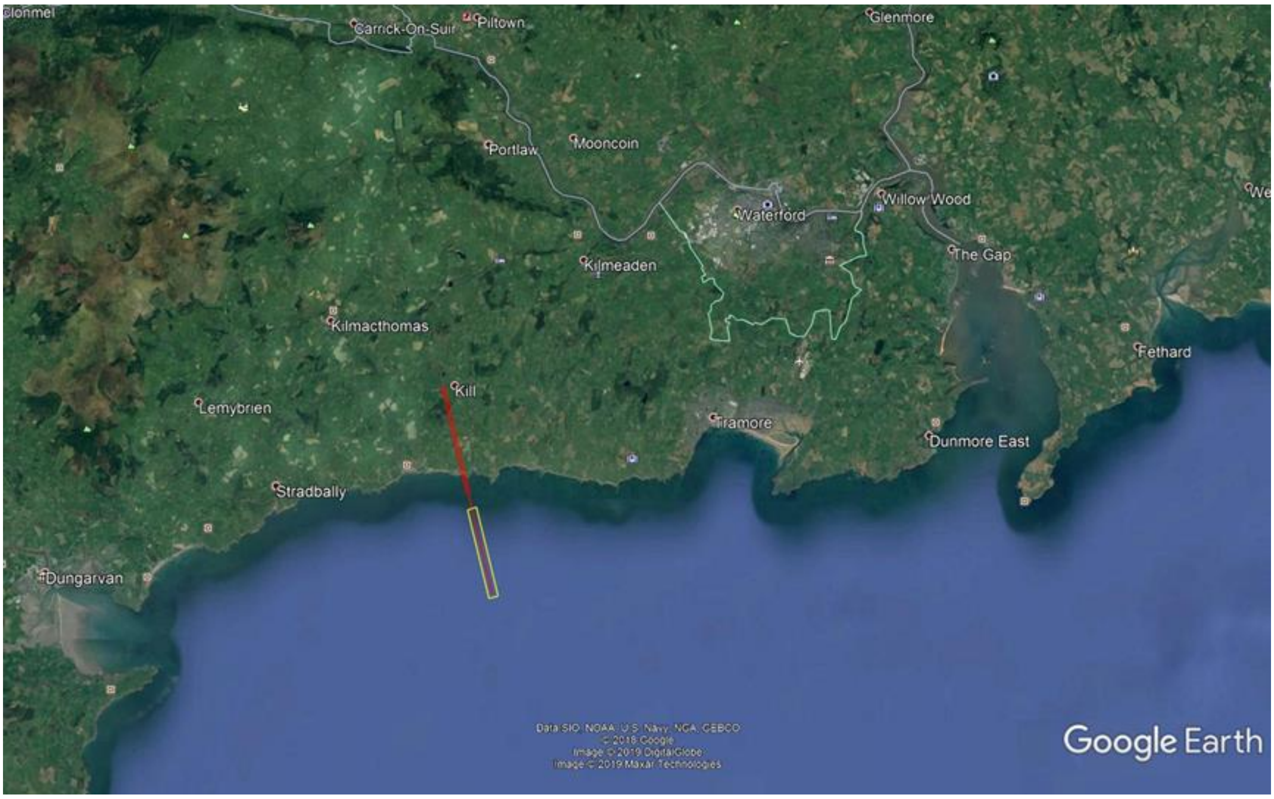

Figure 6. Waterford land/seawater test line location (red line, deep sea section indicated by yellow box).

3.8 Altimeter Calibration

The altimeter calibration test is carried out to ensure proper functioning of the aircraft altimeters. This is done by flying over a flat surface (runway or water body) at a series of different elevations. A correlation coefficient can then be calculated with values greater than 0.97 indicating an accurate calibration result. This test was performed on June 9, 2020 at the Gatineau Airport, Gatineau, QC. Five passes were conducted over the runway at heights from 40 to 120 m above ground at various levels. The altimeter values were compared to the post-flight differentially corrected GPS altitude information for calibration. An ideal altimeter would yield a slope of 1 and an intercept of 0. The Collins radar altimeter slope was 0.9990 and the intercept -0.6215 m. The laser altimeter slope was 1.0020 and the intercept was 0.1228 m. These results are within the expected accuracy of the altimeters

3.9 Mobilisation

The contractor SGL survey aircraft arrived at Waterford airport for the A8 and A9 surveys on 23rd August 2020 and the crew continue 14 days of self-isolation due to Covid19. The first production flight for A8 was undertaken on 20/08/2020 and completed on 15/07/2021. A total of 96 flights were flown over A8 block. The A9 survey was continued immediately at the completion of A8 block. The first production flight for A9 block was commenced on 25/07/2021 and the final flight completed on 21/09/2021. Remobilisation of the field crew was delayed in 2021 again due to the effects of Covid-19. A total of 46 flights were flown over A9 block. The aircraft demobilized in the last week of September 2021.

3.10 Test Line

As part of on-going calibration testing and to help with the integration of different datasets collected during different seasonal conditions, a test line was developed (2011-2019) at Donegal Bay. However, a new test line was established in 2019 just south of Waterford, with the first test flown on 22nd April 2019 for A7 block.

The same test line (Figure 6) was flown in 2020 and 2021 for A8 and A9 blocks. This new test calibration line was established close to the Village of Kill, Co. Waterford in the south of Ireland about 20 km to SW of Waterford city (see Figure 6). The test line is located between 646290 m E & 597625 m N and 644865 m E &, 602937 m N in ITM coordinate system. The Test line is 5.5 km long (4.5 km on land, 1 km over the sea).

3.11 Personnel

Members from both SGL and the Tellus team were involved in the airborne geophysics operations, the main personnel are listed below in Table 7 and 8.

Table 7: SGL Field Crew.

Personnel	*Name*	*Dates on field*
Operations Manager	Kevin Charles	n/a
Field Crew Chief	Alison McCleary	June 15, 2019 – September 15, 2019
Data Processor	Angella Farr	October 12, 2020 – December 14, 2020
Technician	Mike Nguyen	August 20, 2020 – October 15, 2020
Technician	Lee Duncan	March 16, 2021 – June 11, 2021

Technician	Zachary Seguin-Forest	June 9, 2021 – July 16, 2021
Lead Pilot	Steve Gebhardt	August 21, 2020 – end of project
Pilot	Charles Dicks	August 21, 2020 – November 19, 2020
Pilot	Charles Dicks	April 14, 2021 – end of project
Pilot	Steven Hyde	August 23, 2020 – December 14, 2020
Pilot	Steven Hyde	June 27, 2021 – end of project
Pilot	Jean Deschenes	May 18, 2021 – July 4, 2021
Pilot	Jeff Tucker	July 12, 2021 – end of project
AME	Dwayne Bailey	August 21, 2020 – December 5, 2020
AME	Dwayne Bailey	April 17, 2021 – end of project

Table 8: GSI Tellus Team.

Field Personnel	***Name***
Head of Programme / GSI Principal Geologist	Ray Scanlon
Project Manager	Dr. James Hodgson
Geophysicist	Mohammednur Desissa Ture
Geophysicist	Dr. Mark Muller
Communications Manager	Emma Scanlon

4.Outreach Programme

4.1 Tellus Public Relations

Due to the low flying nature of the survey (nominal survey altitude of 60 m), the distribution of population centres and land use within the survey area, an extensive outreach programme was undertaken. This comprised a comprehensive information campaign including meeting with local stakeholders, interviews on local radio, articles in both national and local newspapers and social media updates. Approximately 172,400 and 160,900 information fliers were posted to land owners within the A8 and A9 survey areas respectively (Emma Scanlon, Pers. com.). State agencies including County Councils, An Garda Síochána and Local Authorities were also contacted and regularly updated on the progress of the survey. Of particular significance was the bloodstock sector with notifications given through the Weatherby's Organisation (thoroughbred horse registrations) and the Irish Thoroughbred Breeders Association. Progress updates and a weekly flight plan was also posted on the Tellus website: www.gsi.ie/tellus.

As part of this outreach programme a web-based, data management software program was used which has been developed internally within the Department. This software, called the Tellus Communications Viewer (TCV), was used to log all enquiries and record all communications with landowners and different stakeholders. Following the outreach programme, any land owners, particularly livestock owners, who required notification of the survey in their area were contacted and their land holding digitised within the TCV. The TCV could then be used to determine which flight lines intersected which landholdings and which people might be affected by the flight. Before each flight, a Tellus team member would contact the SGL party chief and identify any land owners who required notification. These people where then contacted, and their responses logged. This allowed stock to be moved or in some cases, a high fly zone (214 m / 700 ft) to be flown above these properties.

High fly zones were also introduced over urban areas (populations greater than 2500) as required under the permit. During survey activities, an "on-call rota" was established to make sure that there was a team member on duty at all times seven-days a week, to deal with urgent enquiries relating to the airborne survey. A free-phone information line (1800 45 55 65) was in operation and was managed by PR company RPS Communications in order to take enquiries about the airborne survey. While the survey was operational, the line was manned during office hours by RPS and out of hours by the Tellus communications representative on call. All calls if required were logged in the TCV managed by the communication and project manager.

5. Quality Assessment

5.1 QA/QC

During the survey operation, data were supplied to the Tellus geophysicists via FTP from SGL on a weekly basis. The data were checked to determine whether it conformed to the required specifications/re-flight requirements as outlined in Section 2.4. The following checks were carried out on all data:

- Terrain clearance and altitude deviations
- Flight line accuracy
- Magnetometer noise
- Ground speed
- Magnetic base station – diurnal variations
- Magnetic noise – Fourth difference/noise
- Gamma ray stability
- EM - noise level, conformity and orthogonality

Weekly QC reports were filed and discussed with the SGL party chief and any required re-flights scheduled into the new flight plan. The weekly QC reports have been collated and can be found as an internal GSI document. Overall, technical specifications were adhered to by the contractor. High altitude deviations, mainly the result of the severe topography in the west, along with induced high fly zones due to urban areas or sensitive livestock areas, were a constant issue.

6. Survey Outputs & Statistics

6.1 Survey Production

The survey consisted of a total of 38,410 and 18,040 km for blocks A8 and A9 respectively. These blocks have been merged with previous survey data. There were 459/59 and 232/39 (traverse/tie lines) for A8 and A9 blocks respectively. A full list of all flight logs and a flight line summary is contained within the SGL Technical Reports (SGL, TR-888-000, 2021).

Table 9: Survey Operation overview.

Airborne Survey Contractor	Sander Geophysics Ltd.
Survey Aircraft:	De-Havilland DHC-6 Twin Otter (C-GSGF)
Survey Base:	Waterford Airport
Aircraft arrival:	23rd August 2020 (Waterford Airport)
Flying dates:	20/08/2020 and completed on 15/07/2021 (A8) 25/07/2021 and completed on 21/09/2021 (A9)
Total no of Flights Productions, re-flights and test flights):	96 (A8) and 46 (A9) flights.
Date of demobilisation:	Last week of September 2021
Total Production km's flown:	(38,410)+(18,040)=56,450 km

The airborne survey operated 7 days a week over 23 production weeks for A8 block. The first four weeks were preparation weeks and 21 weeks were associated with a winter break from December 2020 to April 2021. The weather provided the main challenge for airborne operations throughout acquisition in the A8 and A9 blocks. The effect of Covid19 also hindered mobilization and demobilization. Rain, poor visibility and windy days caused various delays and aborted flights.

It is seen that week 6 (20/09/2020-27/09/2020) and week 44 (16/06/2021-20/06/2021) delivered the largest line-km per week in the A8 survey (3596 and 3852 km respectively). During A9 survey the largest weekly line-km was recorded in week 6 (23/08/2021-29/08/2021), which was 3442 km.

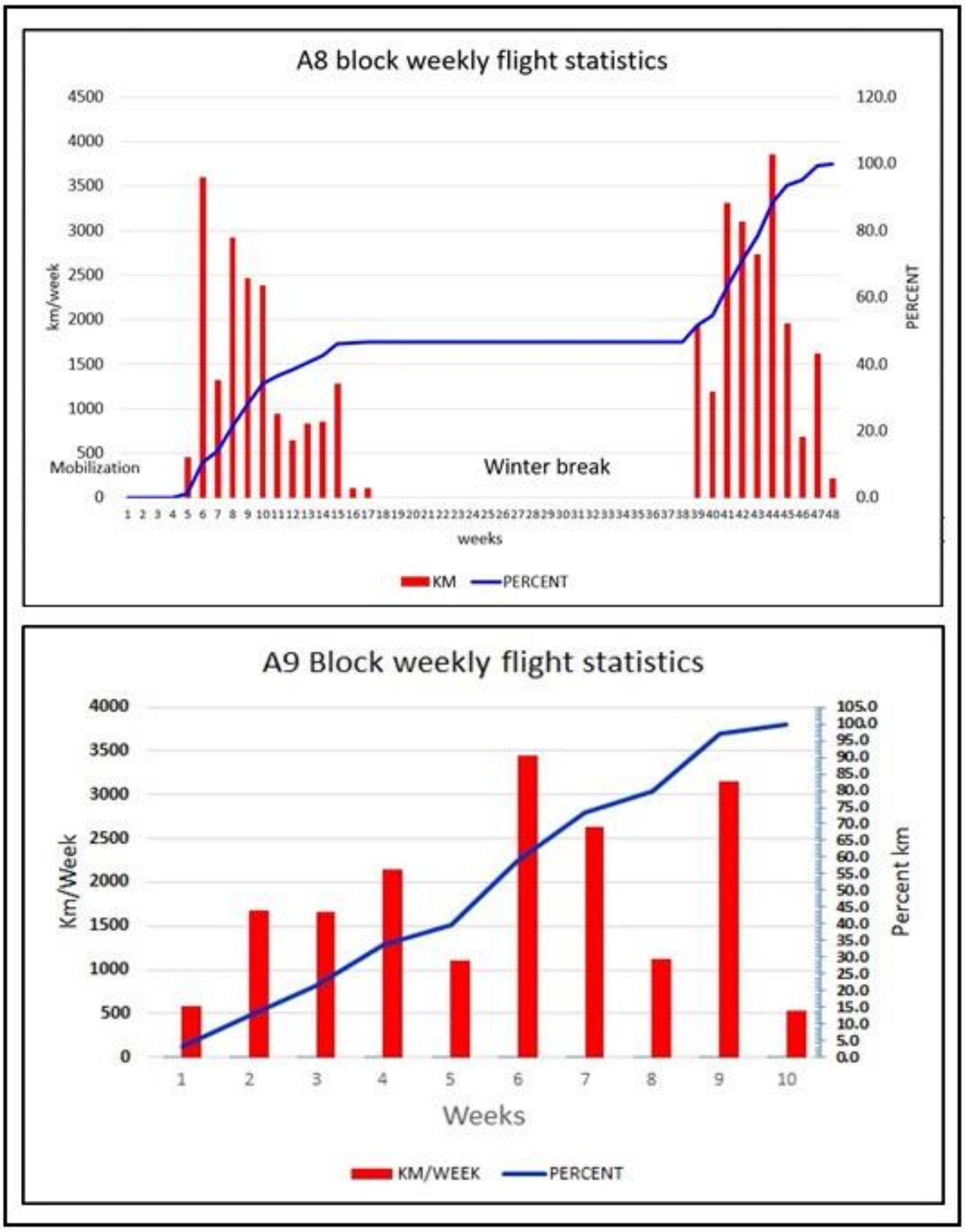

Figure 7: A8 (top) and A9 (bottom) weekly survey production in line-km per week. Week 6 and 44 show the largest weekly flight km in A8 survey block, while week 6 indicated largest weekly km in A9 survey block.

6.2 Altitude

The survey specifications set a survey altitude of 60 m over rural areas and 214 m over high fly polygons and 305 m over built up /urban areas. Topography and land-use in the area of A8 is a mix of low-lying peat bog and undulating grass farmland with significant topography in the north-eastern part.

Table 10. Altitude variations for survey block A8.

Block	Altitude range	max	Mean	SD	# data	%
A8	< 100 m	99.9	65.96	9.42	4,461,473	77.9
	100-120	119.99	109.15	5.75	228,554	3.7
	120-130	129.99	124.83	2.88	83,034	1.3
	130-150	149.99	139.6	5.8	134,196	2.1
	> 150	914.71	258.79	87.62	756,188	14.96

Table 11. Altitude variations for survey block A9.

Block	Altitude range	max	Mean		SD	# data	%
A9	< 100 m	99.9	67.51		9.81	2,250,417	76.8
	100-120	119.99	108.94		5.82	93,505	3.19
	120-130	129.99	124.88		2.89	33,146	1.13
	130-150	149.99	139.6		5.8	53,770	1.83
	> 150	662.17	266.06		89.08	498,552	17.01

The Tellus A8 & A9 surveys operated an extensive outreach programme within the survey area, in particular identifying livestock owners, stud farms and farmers to make them aware of the low flying survey. A number of livestock/horse owners requested that the high fly altitude of 214 m be carried out over their lands. Along with these zones, high fly zones were also identified over towns with populations greater than 2,500, where the flight altitude was kept to 305 m. This resulted in a number of high fly (≥ 214 m) zones throughout the survey area. The high fly zone in A8 block, greater than 150 m, covers about 15% of the survey area (Table 9). In A9 block, the high fly zone greater than 150 m covers 17% of the area. Numerous other altitude deviations were encountered, generally relating to steep terrain over the mountains in the survey area. These high fly zones have had a significant impact in the overall altitude values across the survey (Figure 8).

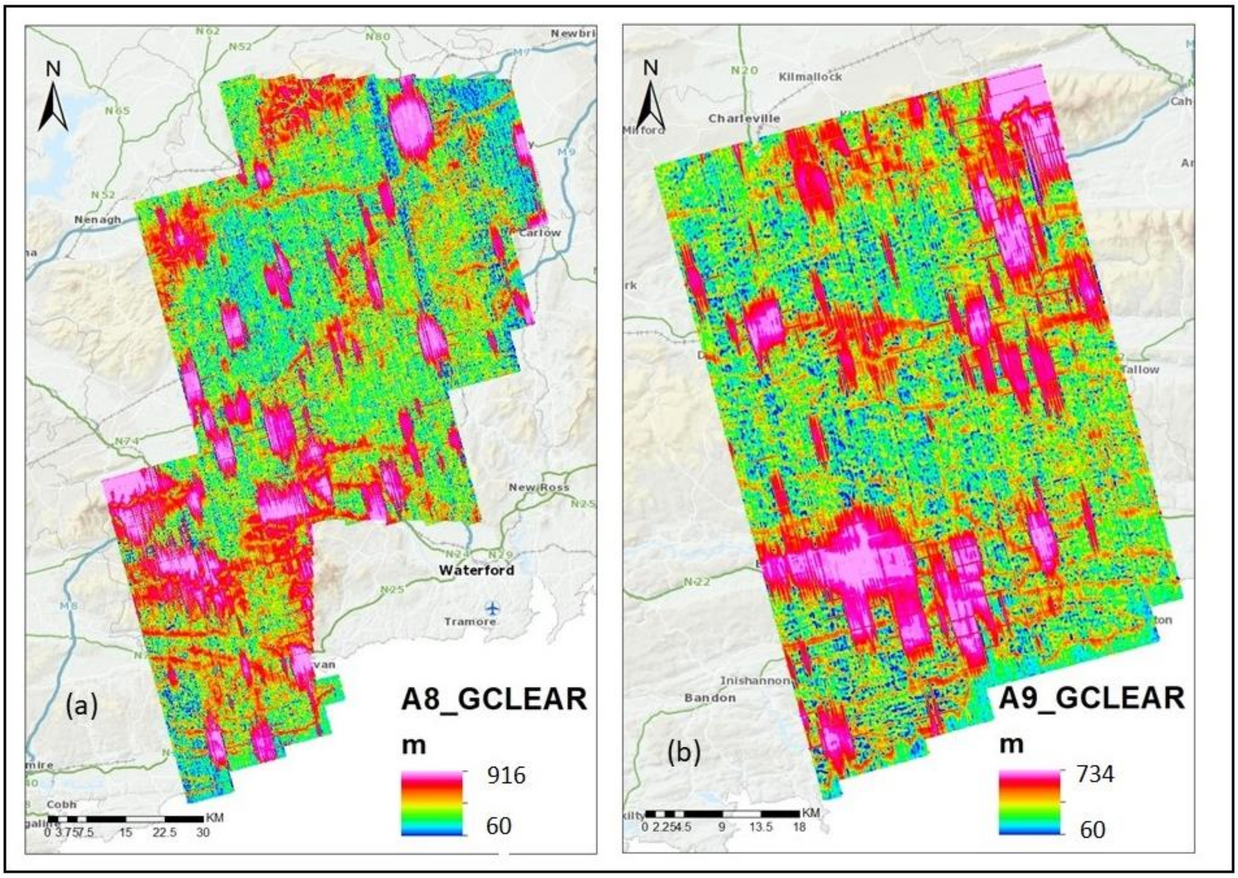

Figure 8: Survey altitude in metres above ground level for Block A8 (a) and A9 (b).

As can be seen from Figure 8, obvious high altitude (pink) zones are observed across the survey areas; these are associated with towns and requested high fly zones but mainly over hilly terrain. The maximum survey altitude recorded was 914 m over A8 block, while the mean over this block is about 98.7 m with a standard deviation of 77.04 m, with approximately 15% of measurements greater than a survey height of 150 m. The maximum survey altitude recorded was 662.17 m over A9 block, while the mean over this block is about 104.60 m with a standard deviation of 83.35 m, with approximately 17% of measurements greater than a survey height of 150 m.

6.3 Magnetic Data Summary

For the magnetic data, a total of 6.184 and 2.929 million data points were collect at a sample rate of 10 Hz for blocks A8 and A9 respectively (including tie lines). The main statistics for the raw and corrected data are summarised below in Tables 12 and 13. Data in the range of magnetic anomalies less than -100 nT and greater than 400 nT are observed to be associated with cultural noise, rather than geological signal.

Table 12: Magnetometer summary statistics for A8 block.

	RAW Magnetic data for A8 block		Compensated, IGRF subtracted and Levelled
BLOCK	DESCRIPTION	NUMBER	NUMBER
A8	No data points	6,184,005	6,184,005
	Sample rate	10 Hz or 0.1 sec	10 Hz or 0.1 sec
	Minimum	48758.54 nT	-231.58 nT
	Maximum	49646.85 nT	561.23 nT

	Mean	49062.22 nT	-26.81 nT
	Standard Deviation	126.36 nT	45.83 nT

Table 13: Magnetometer summary statistics for A9 block.

	RAW Magnetic data for A9 block		Compensated, IGRF subtracted and Levelled
BLOCK	DESCRIPTION	NUMBER	NUMBER
A9	No data points	2,929,409	2,929,409
	Sample rate	10 Hz or 0.1 sec	10 Hz or 0.1 sec
	Minimum	48457.48 nT	-419.85 nT
	Maximum	49581.36 nT	686.56 nT
	Mean	48897.06 nT	-44.38 nT
	Standard Deviation	65.22 nT	21.85 nT

Grids of the resultant magnetic anomaly for A8 and A9 blocks is shown in Figure 9. The data are gridded using the minimum curvature method and a grid cell size of 50 m. Slight differences in the gridded minimum and maximum exist due to grid expansion effects.

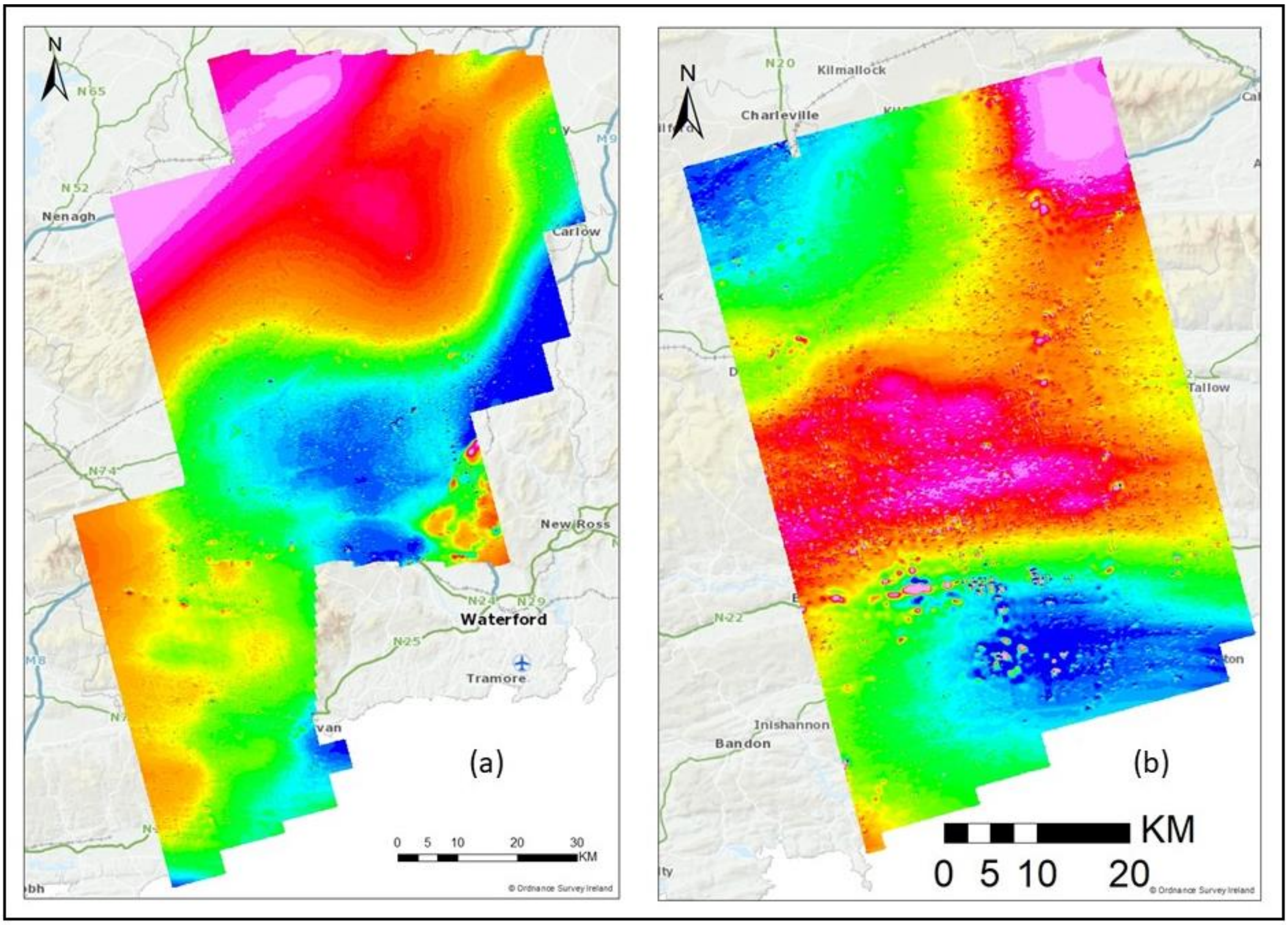

Figure 9: Residual magnetic anomaly for the A8 (a) and A9 (b) blocks. High amplitude (positive) values shown in red and low amplitude (negative) values shown in blue.

6.4 Radiometric Data Summary

For the radiometric data a total of 561,403 and 265,816 data points (excluding tie lines) were collected at a sample rate of 1 Hz for blocks A8 and A9 respectively. The main statistics for each element are summarized below in Table 14, where all data have been corrected and limited to values greater than zero.

Table 14: Corrected and clipped-to-zero radiometric data summary statistics.

	A8 block				A9 block			
Channel	**Min**	**Max**	**Mean**	**SD**	**Min**	**Max**	**Mean**	**SD**
Potassium – RAW (C/S) ("R_POT")	20.00	935.78	222.73	92.33	27.00	679.39	258.33	111.17
Potassium – corrected (%K) ("C_POT_DL")	**0**	**4.62**	**1.01**	**0.42**	**0**	**3.35**	**1.21**	**0.45**
Thorium – RAW (C/S) ("R_THO")	2.00	183.14	56.37	22.14	3.00	191.12	68.32	28.33
Thorium – corrected (eTh) (ppm) ("C_THO_DL")	**0**	**16.91**	**4.68**	**1.97**	**0**	**15.21**	**5.95**	**2.31**
Uranium – RAW (C/S) ("R_URA")	2.67	192.12	54.24	19.11	2.00	321.25	60.93	21.76
Uranium – corrected (eU) (ppm) ("C_URA_DL")	**0**	**8.1**	**0.88**	**0.33**	**0**	**6.92**	**0.91**	**0.33**
Total Counts – RAW (C/S) ("R_TOT")	365.00	6827	2250.18	829.66	372.01	7140.90	2568.15	996.40
Total Counts – corrected (C/S) ("C_TOT_DL")	**0**	**5924.00**	**1884.34**	**676.10**	**0**	**6590.00**	**2196.62**	**759.27**

Grids of total counts, percentage potassium, equivalent thorium and equivalent uranium are shown below in Figures 10-13 for blocks A8 and A9. Data were gridded using the Inverse Distance Weighted Gridding method and use a grid cell size of 50 m. No clipping of data due to high fly altitudes has been carried out.

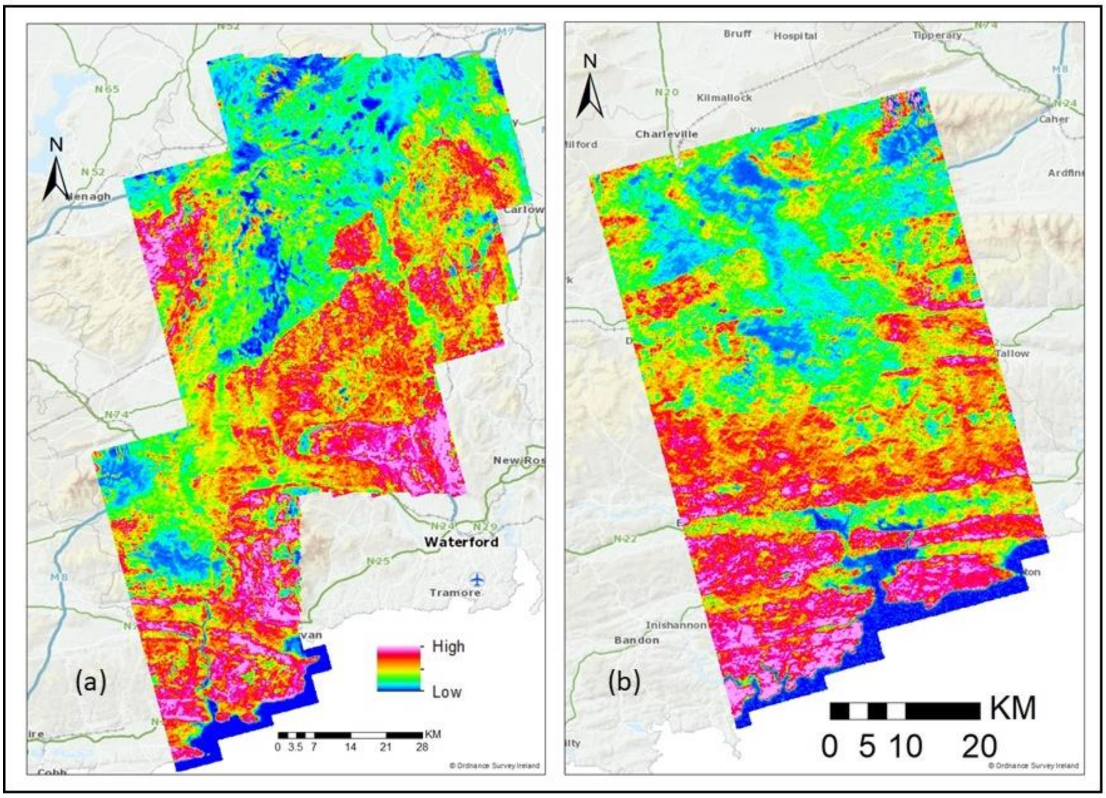

Figure 10: Corrected total count values for the A8 (a) and A9 (b) blocks in counts per second. Offshore areas are not clipped.

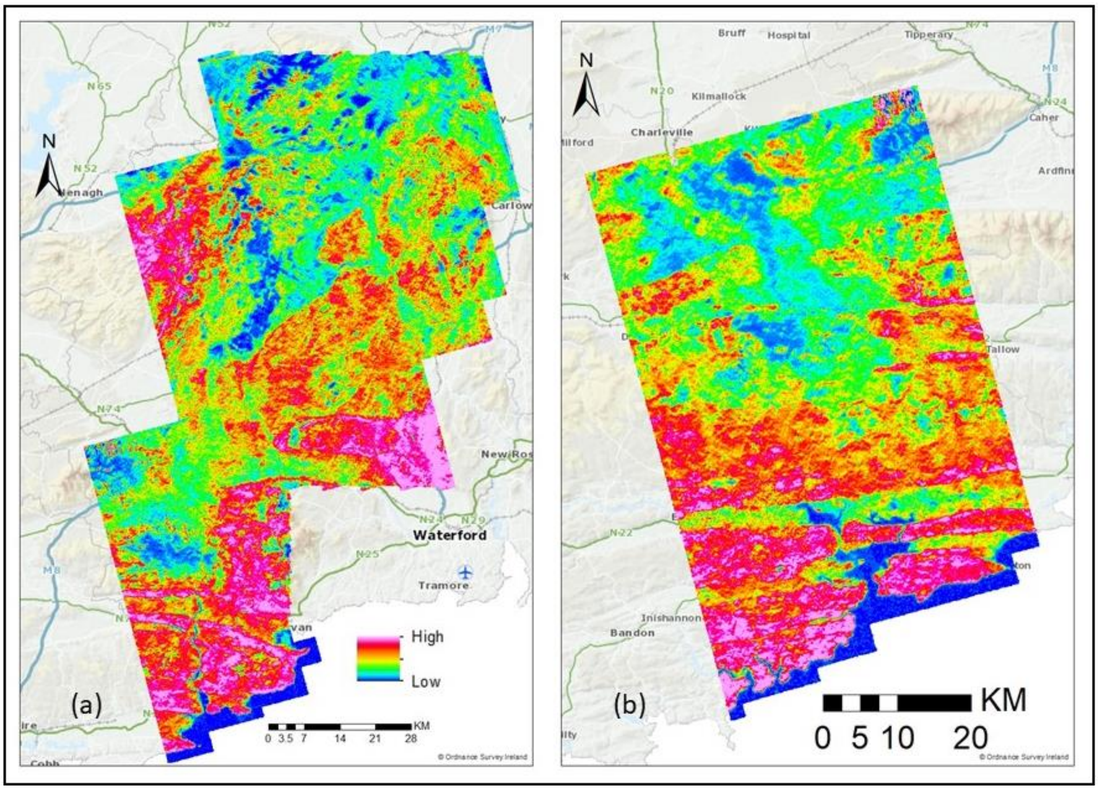

Figure 11: Corrected potassium concentrations for the A8 (a) and A9 (b) blocks as percentage. Offshore areas are not clipped.

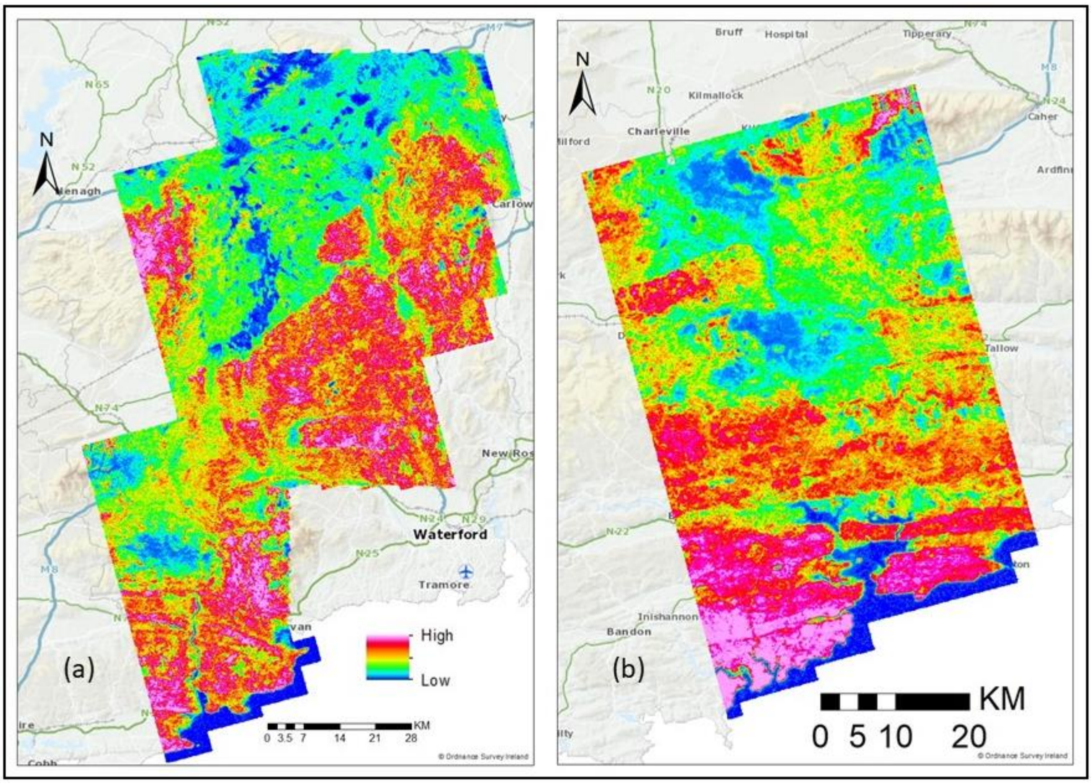

Figure 12: Corrected equivalent Thorium concentrations for the A8 (a) and A9 (b) blocks in parts per million. Offshore areas are not clipped.

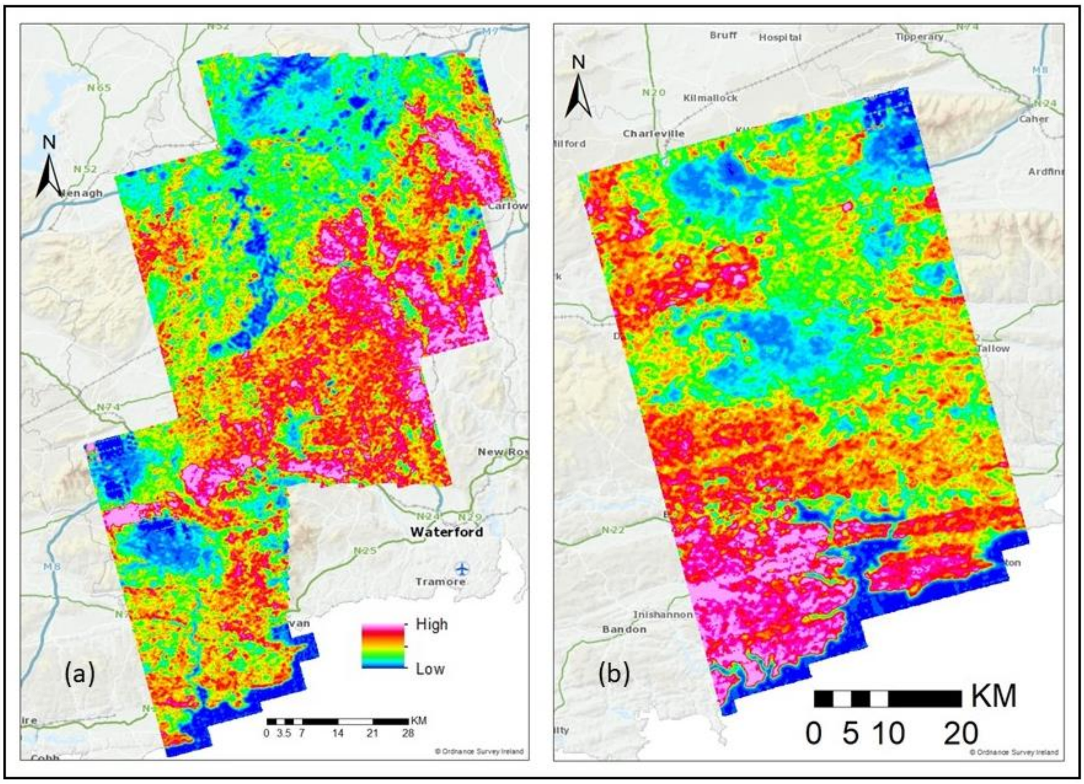

Figure 13: Corrected equivalent Uranium concentrations for the A8 (a) and A9 (b) blocks in parts per million. Offshore areas are not clipped.

6.5 Frequency Domain Electromagnetic (FEM) Data Summary

A total of 6,178,452 FEM data points were collected for block A8 including tie lines, at a sample rate of 10 Hz, i.e., measurements at approximately 6 m intervals along flight lines. In EM processing, the tie line data are not used since EM is a focused signal and is directionally dependent. When tie lines are excluded the number of data points on traverse lines is 5,611,596 for A8 block and these data points were used in the final processing. A total of 2,929,409 and 2,657,571 data points, with and without tie lines, were acquired in A9 block. High fly zones significantly affect the quality of the data. Approximately 15 and 17 % of the data were measured at a survey altitude greater than 150 m (Table 9 and 10) for Blocks A8 and A9 respectively, and therefore may be of limited use. Raw, filtered and levelled in-phase and quadrature component data for each of the 4 frequency channels were delivered for each measurement location. Apparent resistivities delivered by the contractor were determined using the Nomogram (look-up table) method, which uses the in-phase and quadrature responses to calculate apparent resistivity and an associate apparent height of the sensor over an assumed conductive, homogeneous half-space. When deriving the resistivity values, minimum in-phase and quadrature values of 20-50 ppm are used to avoid erroneous results from data below the noise threshold. If the minimum limit is reached the value is capped at the frequency, e.g., 912 Ohm-m for 912 Hz data. Data are also limited to 0.1 Ohm-m. Finally, levelling and micro-levelling of the apparent resistivities is carried out. Full details of the processing of the delivered FEM data for the A8 and A9 blocks can be found in SGL reports (TR-888-000, 2021). The main statistics for contractor supplied FEM data are summarised below in Table 15.

Table 15: Final in-phase, quadrature and apparent resistivity summary statistics for A8 and A9 blocks (traverse lines only).

Block		Levelled mean ppm values		Apparent resistivities (ohm-m)		
	Freq. (Hz)	In-phase	Quadrature	Min	Max	Mean
A8	912	154.69	170.54	0.1	912.00	205.95
	3005	296.85	367.46	0.1	3005.0	224.98
	11962	634.16	639.01	0.1	11962.0	375.19
	24510	897.84	648.31	0.1	24510.0	455.86
A9	912	233.63	178.26	0.1	912.0	191.08
	3005	372.20	376.30	0.1	3005.0	185.20
	11962	669.44	699.35	0.1	11962.0	417.84
	24510	859.95	709.54	0.1	24510.0	552.39

As can be seen from Table 15, the mean in-phase values increase with increasing frequency, which is the expected trend of data. A significant number of flights were conducted over the sea, however, the data of Table 15 have not been clipped to exclude the offshore areas.

Figure 14 below shows the grid of apparent resistivity from the 3 kHz channel for blocks A8 and A9. Data are gridded using the minimum curvature method using a grid cell size of 50m.

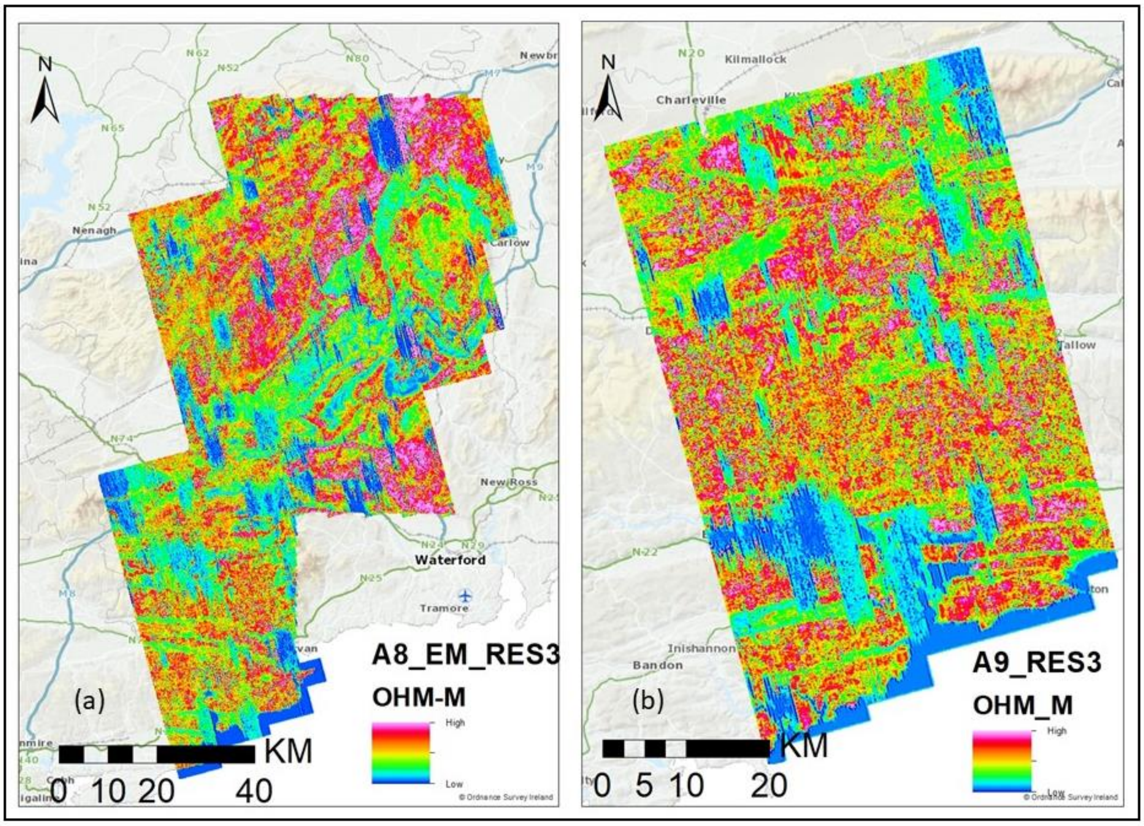

Figure 14: Apparent resistivity (contractor delivered) derived from 3 kHz data for blocks A8 (a) & A9 (b) in Ohm-m. The effect of high-fly (as spurious, low resistivity areas) is clearly observed on both grids.

7. Data Processing

7.1 Introduction

Standard processing was carried out on all three datasets (1: Magnetics, 2: Radiometrics and 3: EM) by the contractor and are discussed in detail by SGL (TR-888-000, 2021). The same processing was adopted as carried out for previous surveys, outlined in Beamish *et al*. (2006) and reviewed in Hodgson and Ture (2013, 2015, 2017), Ture, Hodgson and Muller (2019). The contractor supplied data in ASCII.xyz and Geosoft grid formats. However, along with the standard processing of the Frequency Domain EM (FEM) data carried out by the contractor (SGL TR-888-000, 2021), additional processing of these data was required to allow merging with previous EM data collected as part of the Tellus Programme, which includes Time-Domain EM (TEM) data.

One of the potential issues associated with the EM data is low signal-to-noise ratios of the in-phase and quadrature measurements, which can result from high fly altitudes, cultural noise or strong magnetic susceptibility effects. Owing to small temperature variations, the zero level of the system can drift and therefore a drift correction is applied to all data. The applied drift correction to the in-phase and quadrature data often results in negative values in areas of low amplitude, low signal-to-noise ratio data. Negative values account for approximately 12.3% and 12.8% of the in-phase component and 6.4% and 6.4% of the quadrature component of the lowest frequency (0.9 kHz) data collected in A8 and A9 blocks respectively. The in-phase component is more significantly affected than its quadrature counter-part in the low frequency data. Negative values may also be present in the high-frequency quadrature data (12 and 25 kHz) over highly conductive seawater, where the quadrature response amplitudes are very low. However, changes in the drift correction protocols used between the different surveys over the course of the Tellus programme (2011 to 2021) has resulted in negative values affecting the different surveys to varying degrees.

The average separations in amplitude between all data components are reasonable for both the A8 and A9 blocks, lying in the range 139 to 337 ppm (i.e., the amplitude separation between the data at one frequency and the data at the immediately higher frequency) (See Table 15). The exception is the separation between the 12 kHz and 25 kHz quadrature component data, which is quite small, ~10 ppm for both A8 and A9 blocks. The separation between 12 and 25 kHz is, however, higher for the total-amplitude attribute, as the in-phase components at these frequencies have greater separation. The average separation between 12 and 25 kHz quadrature data is increased when offshore data are clipped from the dataset (See Table 16). Nevertheless, as the baselines of all data components are re-evaluated on an on-going basis, it is anticipated that the average separations between all components (i.e., the baselines) will be optimised (by moderate shifts) on completion of the Tellus programme.

A grid of the power line monitor data channel reveals an extensive network of power line infrastructure across the survey areas (Figure 15). The FEM data may be variably affected by the power lines, depending on, for example, the orientation of the power lines with respect to the flight line direction. The effect of power lines looks minimal on both A8 and A9 data.

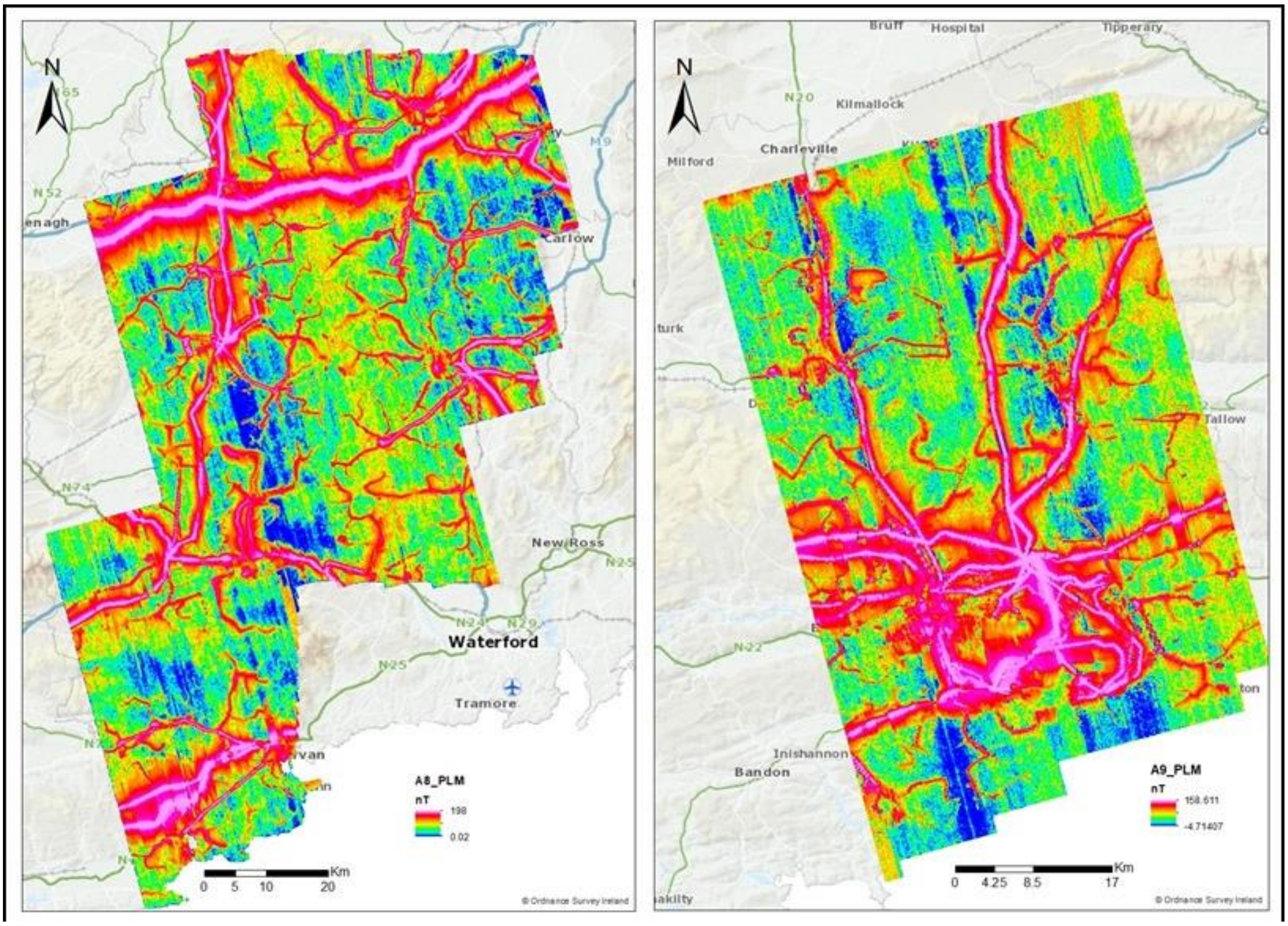

Figure 15: Powerline monitor map for A8 (left) and A9 (right) Blocks.

Variations in derived apparent resistivities, along with differences between time domain and frequency domain derived values, meant that additional processing of the EM data was required before all data could be merged into a single dataset. Moreover, all EM frequency domain data in the Republic of Ireland consist of four frequencies (912, 3005, 11962 and 24510 Hz), while part of the data collected in NI in 2005 consists only of the middle two frequencies (3005 and 11962 Hz). Hence, two different merged data sets are needed:

1. Four frequency merged data for the Republic of Ireland and
2. Two frequency merged data for the island of Ireland

7.2 EM data processing before merger

As discussed, slight variations exist between delivered EM data from the different survey phases. Reviewing the mean values of the in-phase and quadrature data from the different survey blocks (Table 16), it can be seen that blocks A1, A2, A4 and A5, A8 and A9 display lower mean quadrature values (<200 ppm) for 912 Hz than that for other survey blocks, possibly due to a higher percentage of the area flown over conductive sea water and higher flight altitudes. These lower values affect the transformed resistivity values, which are indirectly proportional to the amplitudes of the signal. Values in Table 16 are taken from the “ppm” delivered contractor data.

Table 16: Mean values of all FEM data. These statistics were calculated from original ppm value without tie lines (top).

Block		NI	CAV	TB	A1	A2	A3	A4	A5	A6	A7	A8	A9
Hz	**Mean ppm**												
912	*P09*	959	161	420	100	354	826	701	113	903	442	167	243
	Q09	687	368	265	156	164	274	187	167	238	152	156	168
3005	*P3*	1396	353	594	217	447	932	804	211	886	438	246	333
	Q3	889	628	513	366	240	343	295	317	185	182	262	248
11962	*P12*	2116	1014	1085	601	711	1138	964	661	927	724	495	559
	Q12	959	1100	769	694	485	683	560	659	231	363	438	483
24510	*P25*	3016	1565	1238	808	897	1531	1125	1082	1211	867	738	700
	Q25	1411	1206	575	491	512	618	630	805	379	444	536	553
	Mean Resistivity (JAC)			**Mean Resistivity (SGL)**									
912		134	173	293	249	292	151	309	232	198	205	226	191
3005		153	411	275	405	590	238	238	220	147	166	224	185
11962		343	798	603	1029	828	374	385	322	350	380	375	418
24510		237	605	2739	4123	1585	439	639	562	284	531	456	552
	Mean Resistivity (GSI) HEM RAW (INVERSION METHOD)												
912		70	166	539	427	425	181	563	348	304	276	348	331
3005		130	340	342	1091	812	286	310	248	181	182	306	255
11962		191	397	529	433	829	264	432	254	185	286	323	307
24510		132	396	1412	650	1192	322	734	469	243	412	450	484

As can be seen from Table 16, resistivity values for A1 block look anomalous for 3, 12 and 25 kHz frequencies (6^{th} column). This is due to the highest percentage of data above 150 m altitude in this block, which is about 19.2%, compared to other blocks.

To make all data compatible for merging and to apply a consistent methodology, it was decided to reprocess all original FEM data to produce new apparent resistivities for all survey blocks. This was done using the Helicopter Electromagnetic data processing and analysis (HEM) software extension in Geosoft. This allows the calculation of apparent resistivities based on in-phase and quadrature values by two methods, nomogram and inversion methods. The newly derived values could then be compared with the contractor supplied data, which used nomograms from their own in-house programme. The same filtering or levelling could then be applied to all data, rather than applying different filtering for different blocks.

Using the HEM extension of Geosoft, new apparent resistivities were derived (Table 16). The HEM software has two different schemes for calculating resistivity from real and imaginary components. These are:

- Nomogram (Grid look up) method
- Inversion method

The nomogram method calculates apparent resistivity, or apparent depth values, from airborne EM data using grid look up nomograms. Both in-phase and quadrature components were used to calculate resistivity values. The gridded nomograms were produced using each frequency value.

The inversion method is used to invert resistivity values from airborne data using the uniform half space model. This is a single pass inversion to half-space model for airborne systems that does not rely on look up tables or nomogram files, but calculates forward models as required, sacrificing speed for flexibility and resolution (HEM V6.2 tutorial and user manual). The inversion works by finding the half-space resistivity that minimizes the error in least square sense between the input and calculated in-phase and quadrature values. Flight height, in-phase and quadrature components, frequency, coil separation and coil orientation are used as inputs for the inversion.

Resistivity values were produced using both HEM methods from in-phase and quadrature components, using a fractional error of 1%. These results were then compared with the resistivity values delivered by the contractors. It was also observed that when the error in the data is beyond the 1% range, or if both the in-phase and quadrature components are negative, the inversion does not return a value. This is in fact preferable to the nomogram method that always returns a value no matter how spurious the input values. Comparison of the different datasets show that the resistivity values produced through the inversion method generally result in smoother and more consistent results and show good correlation with the mapped geology (Figures 16 & 17, for example).

As can be seen from comparison of Figure 16 (nomogram method by the contractor) and Figure 17 (HEM inversion method), the inversion transformed resistivity models show clear geologic boundaries and structures compared to nomogram derived resistivity map, although strong edge effects are seen particularly at coastal margins and a greater degree of signal smoothing occurs reducing resolution in places.

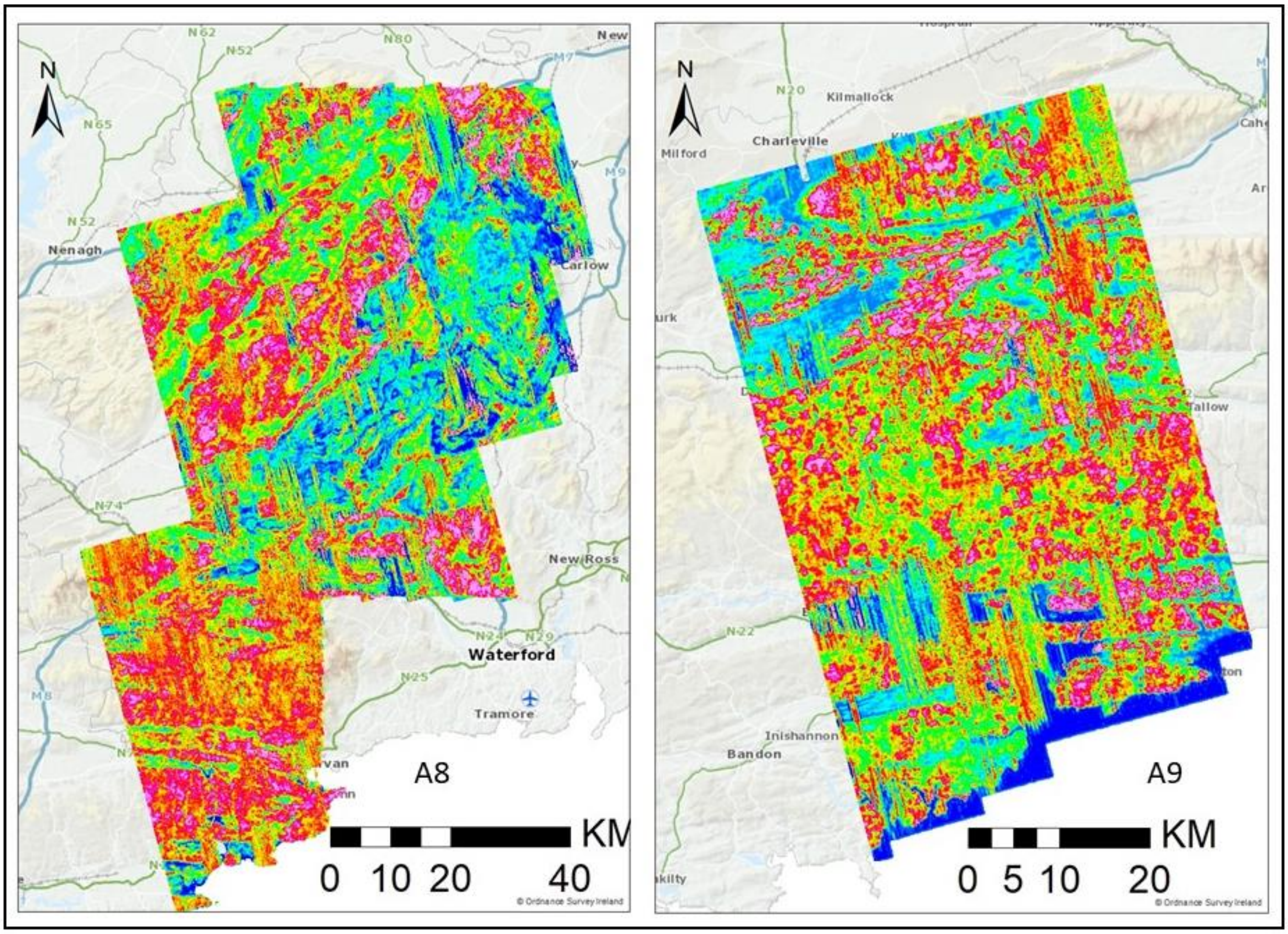

Figure 16: Final apparent resistivity in Ohm-m for 25 kHz delivered by contractor for block A8 (left) and A9 (right) blocks.

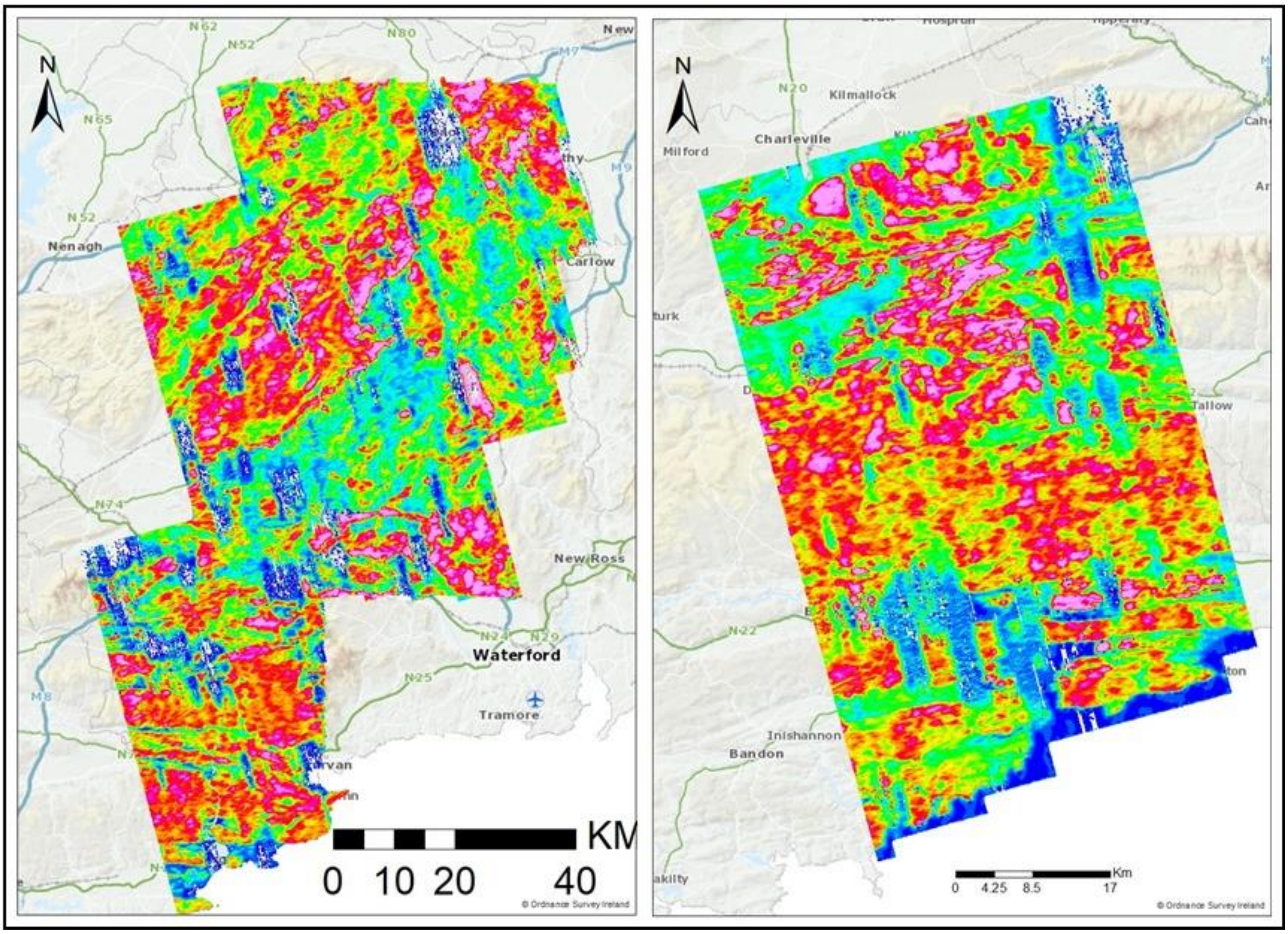

Figure 17: Levelled apparent resistivity in Ohm-m for 25 kHz derived from HEM inversion method for A8 (left) and A9 (right) blocks. The white spaces in the grid are where the inversion didn't return values.

7.3 Noise reduction of FEM data

Negative and very small positive amplitudes of both in-phase and quadrature values have been shown to produce erratic or no resistivity values. All data were clipped to 20 ppm to reduce noise levels for both in-phase and quadrature components. The statistical distribution of the data shows that more than 99% of the data are within the range of 0-2500, 0-2500, 0-2000 and 0-2500 ohm–m for 0.9, 3, 12 and 25 kHz respectively for levelled HEM resistivities for block A8. It was also seen that the statistical distribution of the data shows that more than 99% of the data fall within the range of 0-2500, 0-1500, 0-1600 and 0-2000 ohm–m for 0.9, 3, 12 and 25 kHz respectively for levelled HEM resistivities for block A9. The negative values are generally related to very low resistivity over seawater or areas of high survey altitude. The data were then clipped to the apparent resistivity range that covers more than 99% of the data (as mentioned above) to remove any spurious values.

Detailed investigations of the control test lines flown at different survey altitudes during each survey phase (Bundoran and Waterford test lines) have shown that data recorded above an altitude of >150 m are less reliable. Therefore, all frequency domain data blocks were clipped for altitudes greater than 150 m. The exception is the Tellus north midlands data (time domain) where the effect of high altitude is minimal.

8. Data Merging Overview

8.1 Master Database

A master database was created from the previously merged data sets and from the newly acquired A8 and A9 blocks, as well as the A6 block. The previous merged data include: Northern Ireland (NI), Tellus Border (TB) Cavan (CAV), Tellus North Midlands (TNM), A1, A2, A3, A4, A5, Waterford and A7 blocks. This previous merged dataset is referred to as *Merge2019B* in this report. The newly acquired A8 and A9 blocks completed in 2021 are situated to the south of the 2019B merged data set. The A6 block (west Cork), which was surveyed in 2016 but has not been merged previously, as it had no overlap with other blocks, is now also merged. The current merge therefore includes the earlier *Merge2019B*, A8, A9 and A6 blocks data and is referred to as *Merge2022*. The area included in *Merge2022* is shown in Figure 18 below.

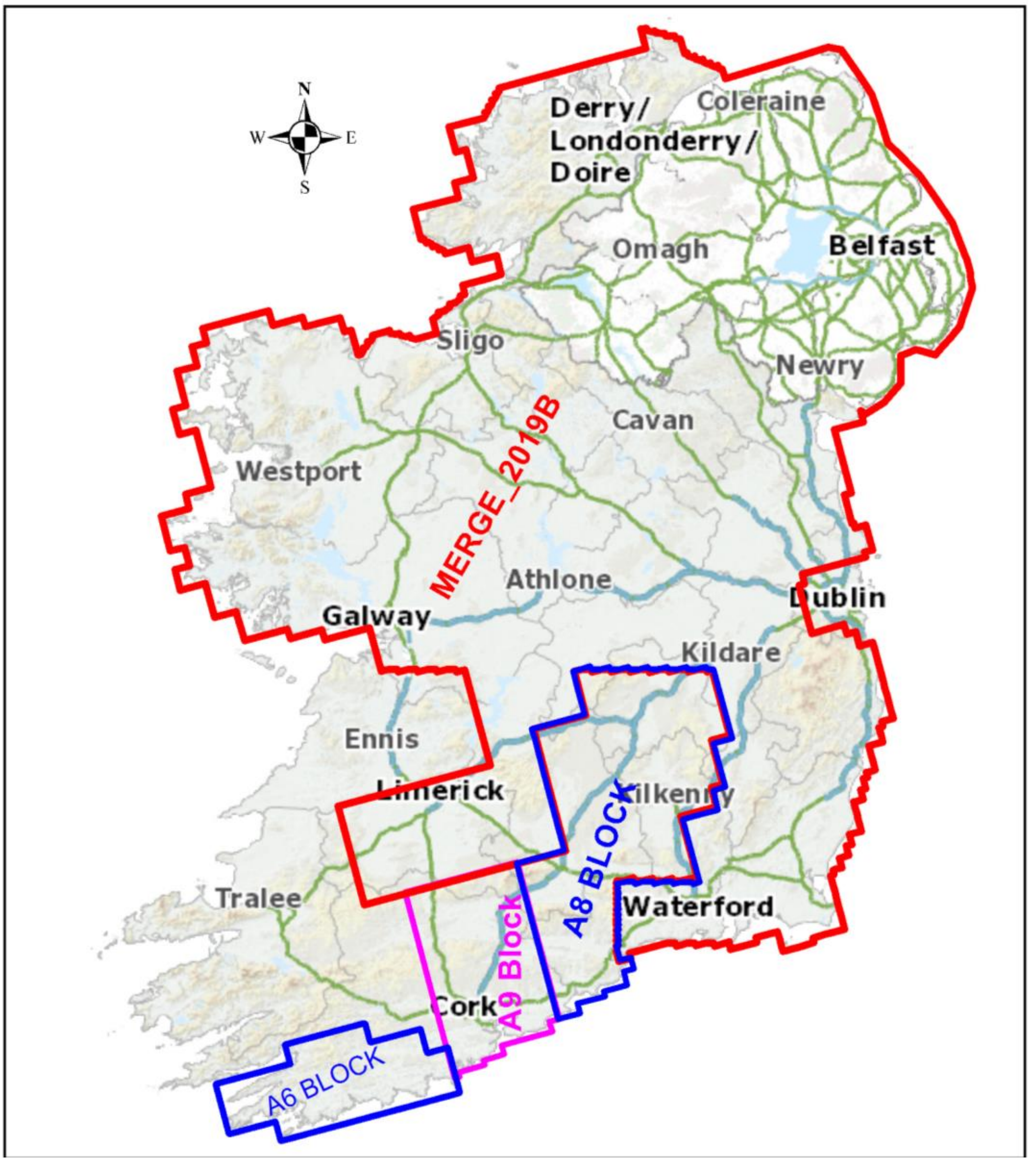

Figure 18: ***Merge2022*** **data. The red polygon shows** ***Merge2019B*** **and the blue and pink polygons represent the latest surveys blocks A8 andA9, as well as block A6, which are to be merged with 2019B.**

Due to the size of the merged data file, a number of channels were removed from the final master database, leaving only the most relevant channels for each database (1) magnetics, (2) radiometrics and (3) electromagnetics. A uniform name was applied to each of the relevant channels for each database.

A Survey ID (SID) channel has been produced to avoid any confusion in identifying the source of the data within the master database, where:

- A9 indicates Tellus A9 data
- A8 indicates Tellus A8 data
- A7 indicates Tellus A7 data
- A6 indicates Tellus A6 data
- A5 indicates Tellus A5 data
- A4 indicates Tellus A4 data
- A3 indicates Tellus A3 data
- A2 indicates Tellus A2 data
- A1 indicates Tellus A1 data
- TB indicates Tellus Border data
- CAV indicates Tellus Cavan data
- TNM indicates Tellus North Midlands data
- NI indicates Tellus Northern Ireland data
- WFD indicates Tellus Waterford data

The A8, A9 and A6 databases were merged with the *Merge2019B data* to produce a single master database referred to as *Merge2022* using the merge database tools in Geosoft. Data were corrected following assessment of gridded data from the overlap zones between separate grid blocks. Grids of the corrected data were then created and then sampled back to the new master database for each relevant channel.

8.2 Co-ordinates

Since 2014, it has been the policy of Geological Survey Ireland (GSI) to use the Irish Transverse Mercator (ITM) co-ordinate system for all mapping. The previous surveys of Northern Ireland (NI), Tellus Border (TB) and Cavan Monaghan (CAV) were delivered using Irish National Grid co-ordinate system. Therefore, all previous datasets were transformed into ITM co-ordinates to match with data from A9, A8, A7, A6, A5, A4, A3, A2, A1, WFD and Tellus North Midlands (TNM) and to conform with the policy of GSI.

Table 17: Summary of ITM co-ordinate system

IRISH TRANSVERSE MERCATOR	
Reference Ellipsoid:	GRS80
Central Meridian	08° 00’ 00” West
Vertical Datum:	Malin Head
Map Projection:	Transverse Mercator (Gauss Conformal)
True origin:	53° 30’ 00” North, 08° 00’ 00” West
False origin:	600 km west, 750 km south of true origin
Scale factor on Central Meridian:	0.999820

8.3 Magnetic Data Merging

Magnetic data from *Merge2019B* (NI, TB, CAV, TNM, A1, A2, A3, A4, A5, A7 and WFD) have been merged with A8, A9 and A6 blocks to form a single dataset for the entire area surveyed to date as part of the Tellus Programme. The detail of *Merge2019B* is found in Hodgson, Ture and Muller (2020) which accompanied the release of the merged dataset on 24th February 2020.

As the airborne surveys continued over the years, each new survey was designed to include an area of overlap with previous survey blocks, therefore assisting in the merge of any new data. Datasets were compared in the regions of overlap, allowing direct comparison. A correction factor was then applied to the older dataset to bring it into line with the most recently acquired data, with the exception of the electromagnetic EM data, which have been levelled to the previously determined Tellus Border data level.

The final levelled residual magnetic data were used to achieve *Mag_Merge2022*. These data have been corrected for magnetic compensation, diurnal variation and IGRF effects and are fully levelled. A grid of the magnetic anomaly was then created for *Merge2019B*, A8, A9 and A6 blocks and the mean differences between the overlapping regions from the three grids were then calculated. The differences were then added sequentially to the older dataset (*Merge2019B*). The final deliveries of A8 and A9 (DLV254 and DLV2420) are seen to be the smoothest boundaries with mean boundary difference of 3.74 nT betwe. Due to smooth boundary between A8 and A9 blocks, these two blocks were first merged together by adding 3.74nT to A9 data. This merge between A8 and A9 is named as m*erge-A8A9_2021A*. The mean difference between overlapping zones of m*erge-A8A9_2021A* and merge 2019B is -57.1 nT. This value was added to *Merge2019B* to produce *Merge2021B-intermediate*. The mean difference between A6 and *Merge2021B-intermediate* is -13.09 nT. This value was added to *Merge2021B-intermediate* to produce *Merge2022* which is the final merged magnetic dataset.

The corrected data were then knitted together using the grid knitting program from Geosoft, using the suture stitching method and an output grid cell size of 50 m. The de-trending method for both grids was set to none. The final fully merged grid was then re-sampled into the Master database using the sample-a-grid function in Geosoft. Figure 19 below shows the gridded result of the merged magnetic database.

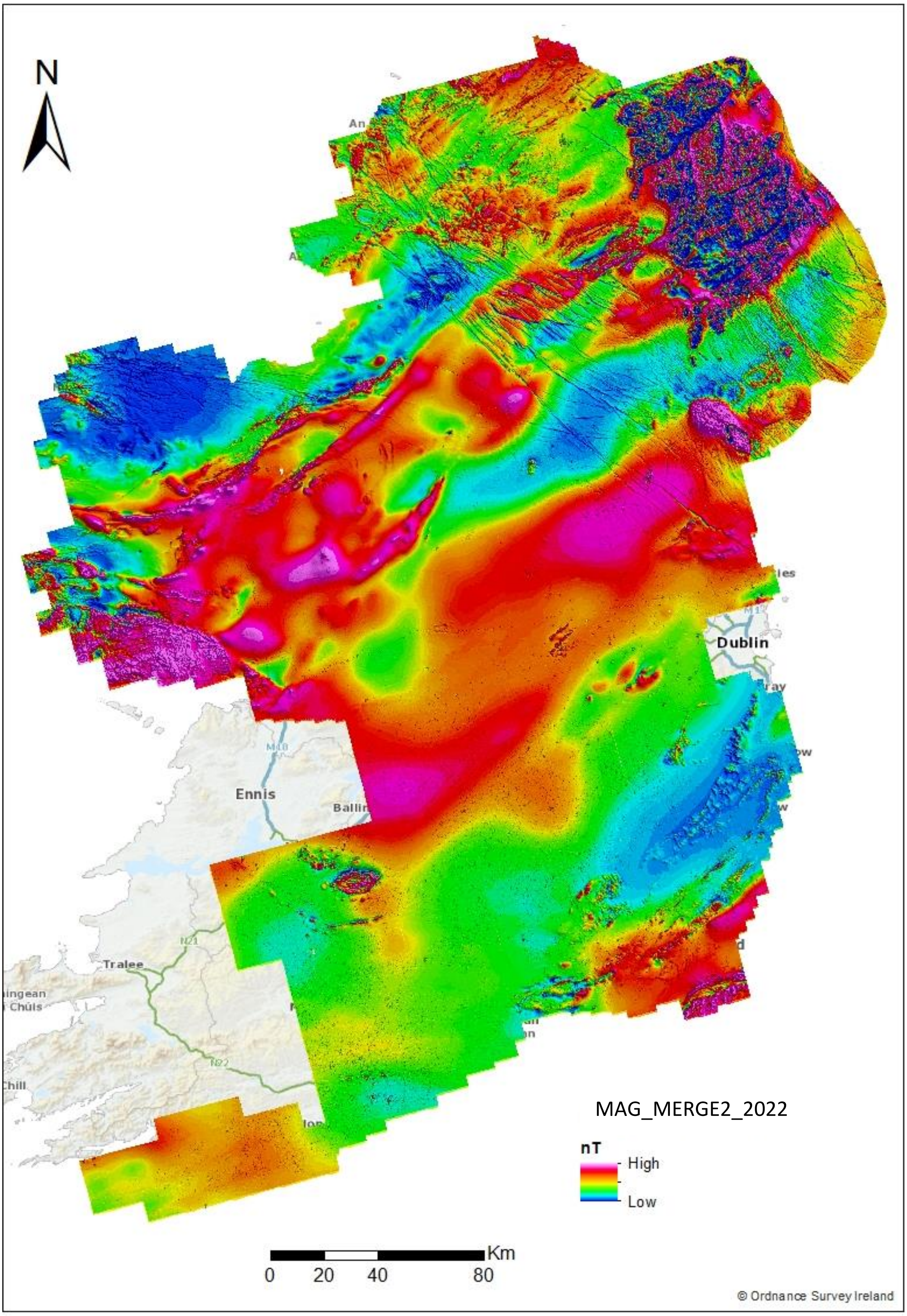

Figure 19: Merged residual magnetic anomaly (*Merge2022*) from *Merge2019B*, A8, A9 and A6 blocks.

8.4 Radiometric Data Merging

Radiometric data from *Merge2019B* (NI, TB, CAV, TNM, A1, A2, A3, A4, A5, A7 and WFD blocks) were merged with A8, A9 and A6 blocks to form a single radiometric dataset (*Merge2022*) for the entire area surveyed to date. Datasets were compared in the regions of overlap and a correction factor for each dataset was established as outlined in the above section. These correction factors were then applied to the older datasets to bring it into line with the most recently collected data. Details of *Merge2019B* are given in Ture, Muller and Hodgson (2020).

Standard processing and corrections to radiometric data were applied by the contractor as stated in IAEA (2003) and Grasty and Minty (1995). A1, A2, A3, A4, A5, A6, A7, A8, A9 and Waterford data were collected using RS-501 spectrometer, while the remaining data were collected by GR-820 Spectrometer.

Table 18: Standard Gamma Ray Energy windows for radiometric survey (IAEA 2003).

Window name	Energy Window	Major peak (keV)	Radio nuclide
Potassium (K)	1370 keV to 1570 keV	1460	K-40
Thorium (Th)	2410 keV to 2810 keV	2614	Tl-208
Uranium (U)	1660 keV to 1860 keV	1765	Bi-214
Total Counts	400 keV to 2810 keV		

Table 19: Energy ranges (channels) used by different Tellus surveys (From 2005-to-date). ROI stands for "Region of Interest" in the radiometric spectrum.

SURVEY	ROI	LOW CHANNEL	HIGH CHANNEL	LOW ENERGY KeV	HIGH ENERGY KeV
NI	TC	34	240	396	2808
	POTASSIUM	117	134	1368	1572
	URANIUM	141	159	1656	1860
	THORIUM	206	240	2410	2808
CAV	TC	35	240	410	2810
	POTASSIUM	117	134	1370	1570
	URANIUM	142	159	1660	1860
	THORIUM	206	240	2410	2810
TB	TC	34	240	396	2808
	POTASSIUM	117	134	1368	1572
	URANIUM	141	159	1665	1860
	THORIUM	206	240	2410	2808
TNM	TC	34	240	396	2808
	POTASSIUM	117	134	1368	1572
	URANIUM	141	159	1656	1860
	THORIUM	206	240	2412	2808
A1	TC	34	240	396	2808
	POTASSIUM	117	134	1368	1572
	URANIUM	141	159	1656	1860
	THORIUM	206	240	2412	2808
WFD	TC	136	936	408	2808
	POTASSIUM	460	524	1380	1572
	URANIUM	556	620	1668	1860
	THORIUM	804	936	2412	2808
A2	TC	136	936	408	2808
	POTASSIUM	460	524	1380	1572
	URANIUM	556	620	1668	1860

	THORIUM	804	936	2412	2808
A3	TC	136	936	408	2808
	POTASSIUM	460	524	1380	1572
	URANIUM	556	620	1668	1860
	THORIUM	804	936	2412	2808
A4	TC	136	936	408	2808
	POTASSIUM	460	524	1380	1572
	URANIUM	556	620	1668	1860
	THORIUM	804	936	2412	2808
A7	TC	136	936	408	2808
	POTASSIUM	460	524	1380	1572
	URANIUM	556	620	1668	1860
	THORIUM	804	936	2412	2808
A6	TC	136	936	408	2808
	POTASSIUM	460	524	1380	1572
	URANIUM	556	620	1668	1860
	THORIUM	804	936	2412	2808
A7	TC	136	936	408	2808
	POTASSIUM	460	524	1380	1572
	URANIUM	556	620	1668	1860
	THORIUM	804	936	2412	2808
A8	TC	136	936	408	2808
	POTASSIUM	460	524	1380	1572
	URANIUM	556	620	1668	1860
	THORIUM	804	936	2412	2808
A9	TC	136	936	408	2808
	POTASSIUM	460	524	1380	1572
	URANIUM	556	620	1668	1860
	THORIUM	804	936	2412	2808

From Table 19 it is clearly seen that the energy windows and number of channels are changed, starting from A2 block. The crystal volume was 32 L and channels were 256 to prior to A1 survey block. The upward looking crystal size was changed to 50.4 L (A1), but with 256 channels. Starting from A2 crystal size was changed to 67.2 L and 12.6 L respectively for downward and upward looking and the raw spectrometer channels were changed to 1024.

Details of all processing procedures and calibrations for the A8 and A9 data can be found in the technical report produced by the contractor (SGL, TR-888-000, 2021) and are consistent with standard processing procedures as outlined by IAEA (2003) and Grasty and Minty (1995).

It was decided that all radio-elements should be corrected to correspond with values measured for the most recent survey, i.e., the A8 and A9 blocks. After comparing data statistics in the overlap zones, correction factors were determined based on calculated means of gridded data. Correction (multiplication) factors were used rather than a simple shift (addition/subtraction) as this better reflects the nature of the radiometric data. Applying a simple subtraction, as applied to the magnetic data, could potentially result in negative concentrations in areas of low values, which would be meaningless. The following correction factors were applied to the *Merged2019B* data to bring these data in line with the data of the A8 and A9 blocks, and subsequently the A6 block (Tables 20 - 22).

Table 20: Radiometric correction factors applied to *Merge2019B* data for data merge with A8 block.

	Mean ratio A8 to *Merge2019B* @ Overlap (a)	**Correction applied to *Merge2019B* Data (b1)**	***Merge2021A* is obtained by gridding data (b1) and knitting it with grids of *Merge2019B* for each nuclide and sample it back into master database for every channel**
Potassium (%k)	1.022	1.022*Merge2019B potassium	
eThorium (ppm)	1.05	1.05*Merge2019B Thorium	
eUranium (ppm)	1.1	1.1*Merge2019B Uranium	
Total Count	1.084	1.084*Merge2019B Total count	

After the intermediate merge of A8 to *Merge2019B*, achieved by applying the corrections shown in column (b1), the intermediate merge *Merge2021A* was created and then compared to A9 block within the overlap zone, as shown in Table 20.

Table 21. Radiometric correction factors applied to intermediate *Merge2021A* data for merge with A9 block.

	Mean Ratio of *Merge2021A* to A9 @ overlap (a2)	**Correction applied to *Merge2021A* data (b2)**	***Merge2021B* is obtained by gridding data (b2) and knitting it with grids of *Merge2021A* (intermediate merge) for each nuclide and sample it back into master database for every channel**
Potassium (%k)	1.1	1.1*Merge2021A	
eThorium (ppm)	1.09	1.09*Merge2021A	
eUranium (ppm)	1.1	1.1*Merge2021A	
Total Count	1.07	1.07*Merge2021A	

After the intermediate merge of A9 to *Merge2021A*, achieved by applying the corrections shown in column (b2), the intermediate merge *Merge2021B* was created and then compared to A6 block within the overlap zone, as shown in Table 21. Applying the corrections shown in column (b3) resulted in the final merged dataset, *Merge2022*.

Table 22: Radiometric correction factors applied to intermediate *Merge2021B* data for merge with A6 block.

	Mean Ratio of *Merge2021B* to A6 @ overlap (a3)	**Correction applied to *Merge2021B* data (b3)**	***Merge2022* is obtained by gridding data (b3) and knitting it with grids of *Merge2021B* (intermediate merge) for each nuclide and sample it back into master database for every channel**
Potassium (%k)	1.07	1.07*Merge2021B	
eThorium (ppm)	1.04	1.04*Merge2021B	
eUranium (ppm)	1.08	1.08*Merge2021A	
Total Count	1.01	1.01*Merge2021A	

Correction factors for total count, potassium, thorium and uranium are deemed acceptable, being close to a value of one, with few outliers observed. Following the application of the correction factors, a new grid was created for each element using the new corrected values. These grids were then merged together using the suture stitching method of the grid knitting program from Geosoft. A cell size of 50 m was used with the de-trending method for both grids set to 'none'. This merged grid was then resampled to the master database.

A final merged grid was created from the master database for each element using the inverse distance weighted method and a cell size of 50 m. This gridding method was employed rather than the minimum curvature method (used for other datasets) as it helps to represent the large footprint from which the radiometric data are determined, rather than from a single point. Figures 21 – 25 below show resultant grids for merged total counts, potassium, equivalent thorium, equivalent uranium and radiometric ternary maps. The comparison of means of %K, eTH and eU for each block is shown in Figure 20. It is seen that WFD data shows highest means for the three nuclides, ahead of A9 block. Waterford records high levels for all three radio-nuclides, in particular for thorium. It appears that thorium concentrations are generally higher towards the south compared to northern and central Ireland.

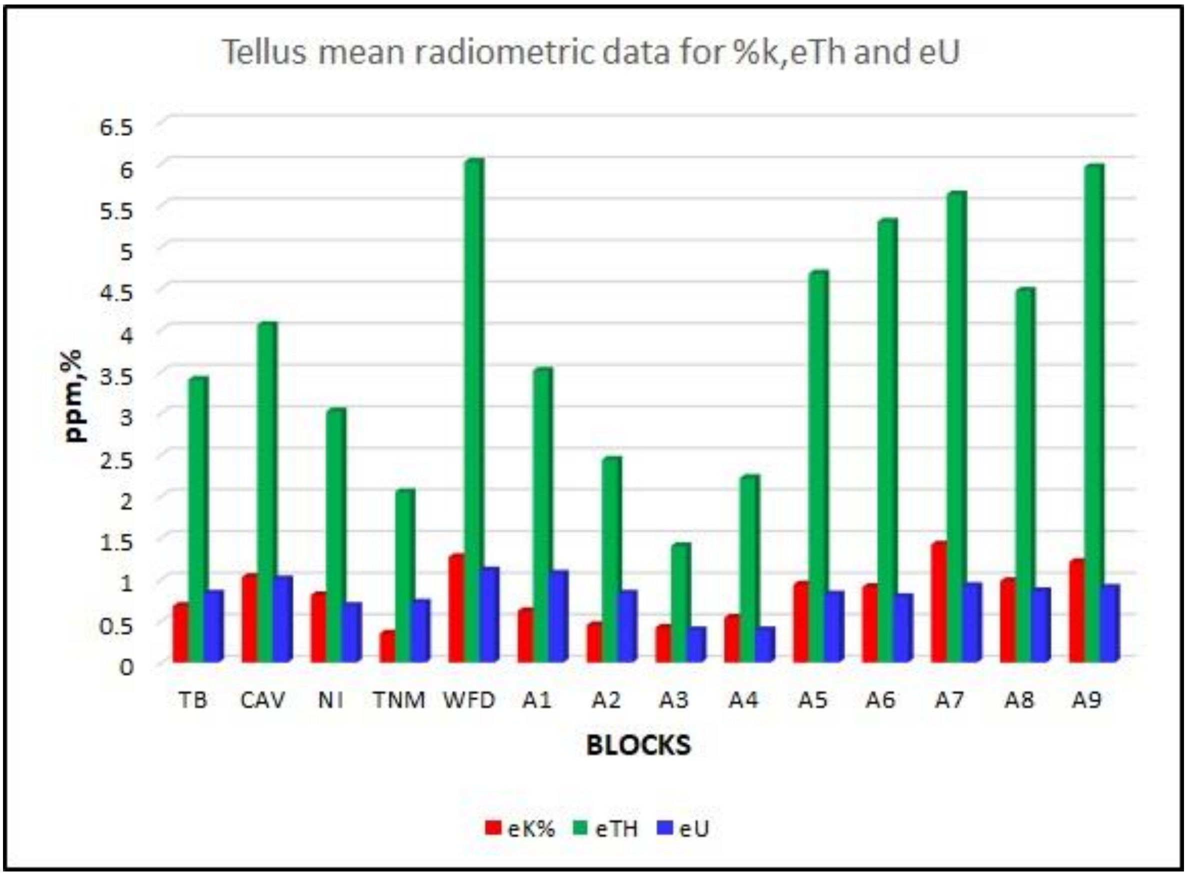

Figure 20: Means of K (%), eTh (ppm) and eU (ppm) for all blocks.

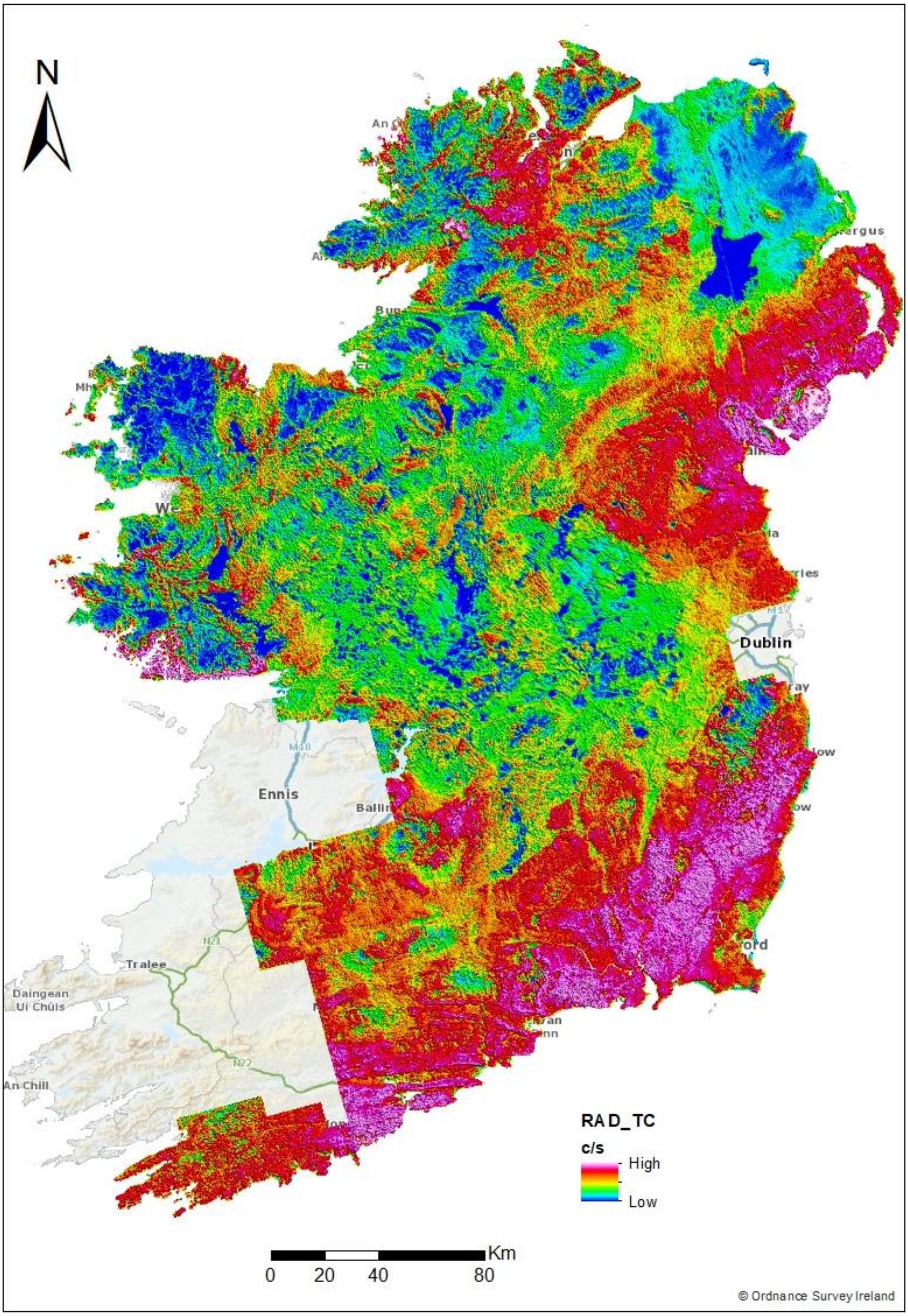

Figure 21: Merged total count radiometric data (cps) from *Merge2019B*, A8, A9 and A6 blocks. This final merge is referred to as *Merge2022*.

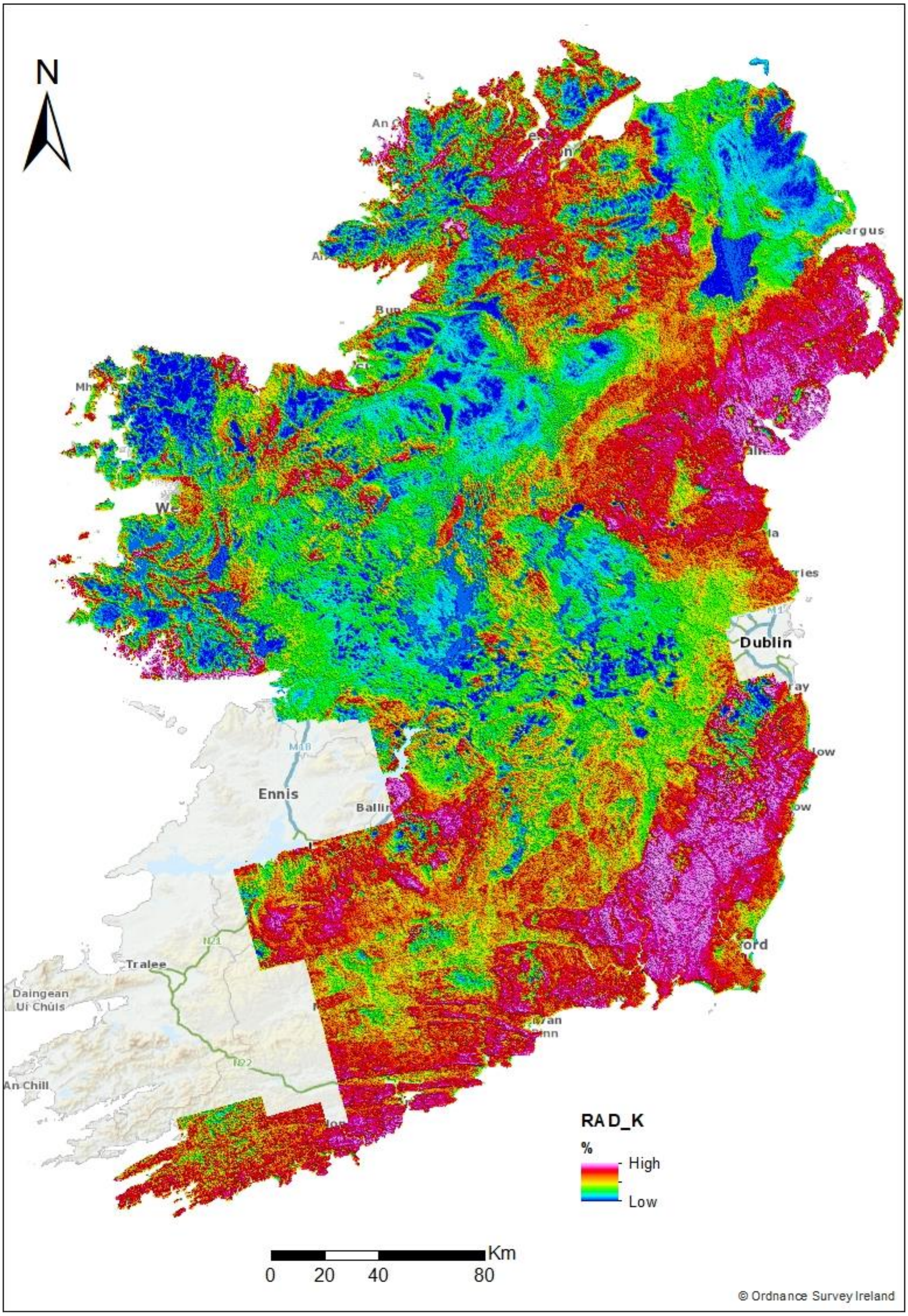

Figure 22: Merged Potassium data (%) from *Merge2019B*, A8, A9 and A6 blocks. This final merge is referred to as *Merge2022*.

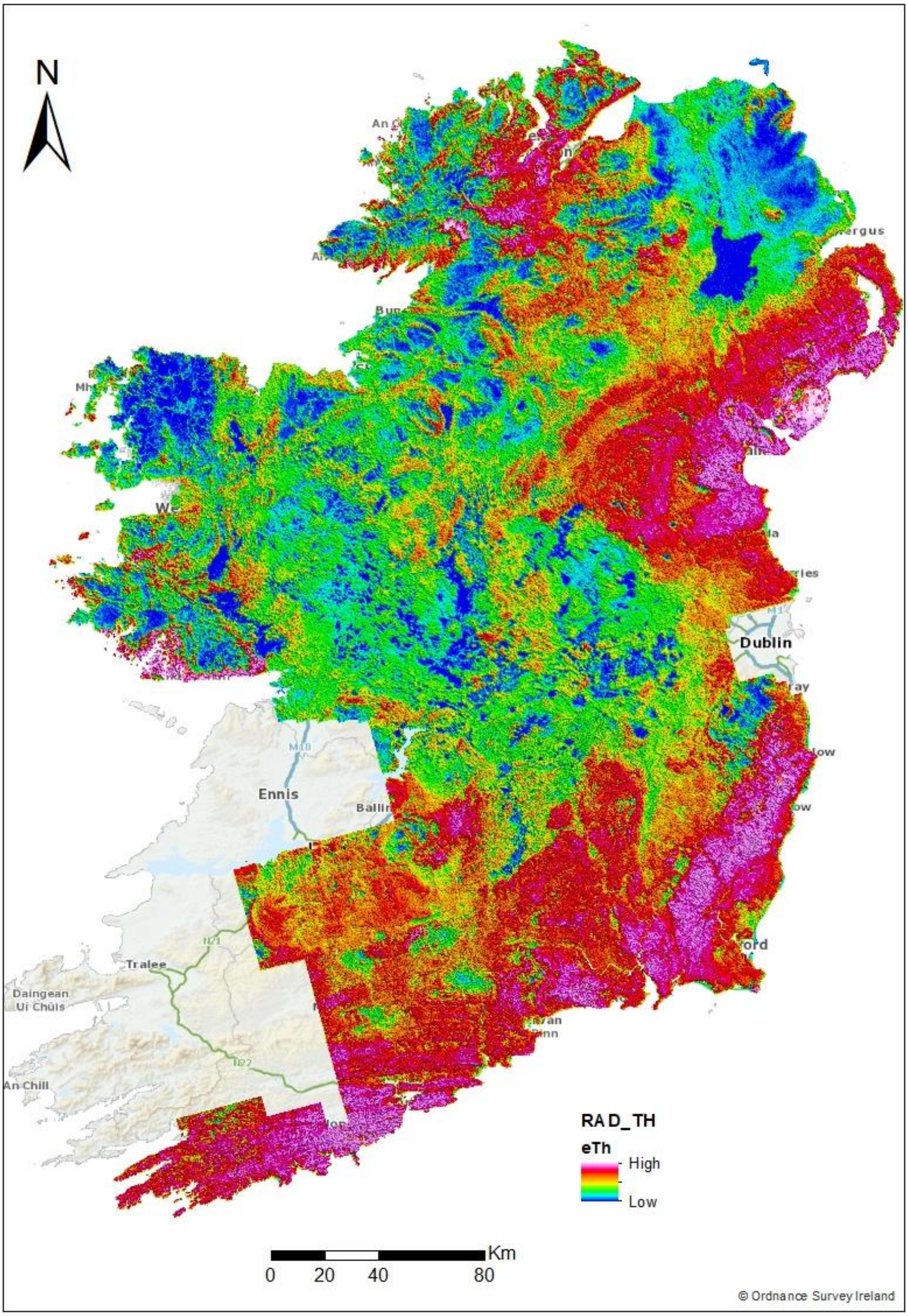

Figure 23: Merged total equivalent Thorium data (eTh in ppm) from *Merge2019B*, A8, A9 and A6 blocks. This final merge is referred to as *Merge2022*.

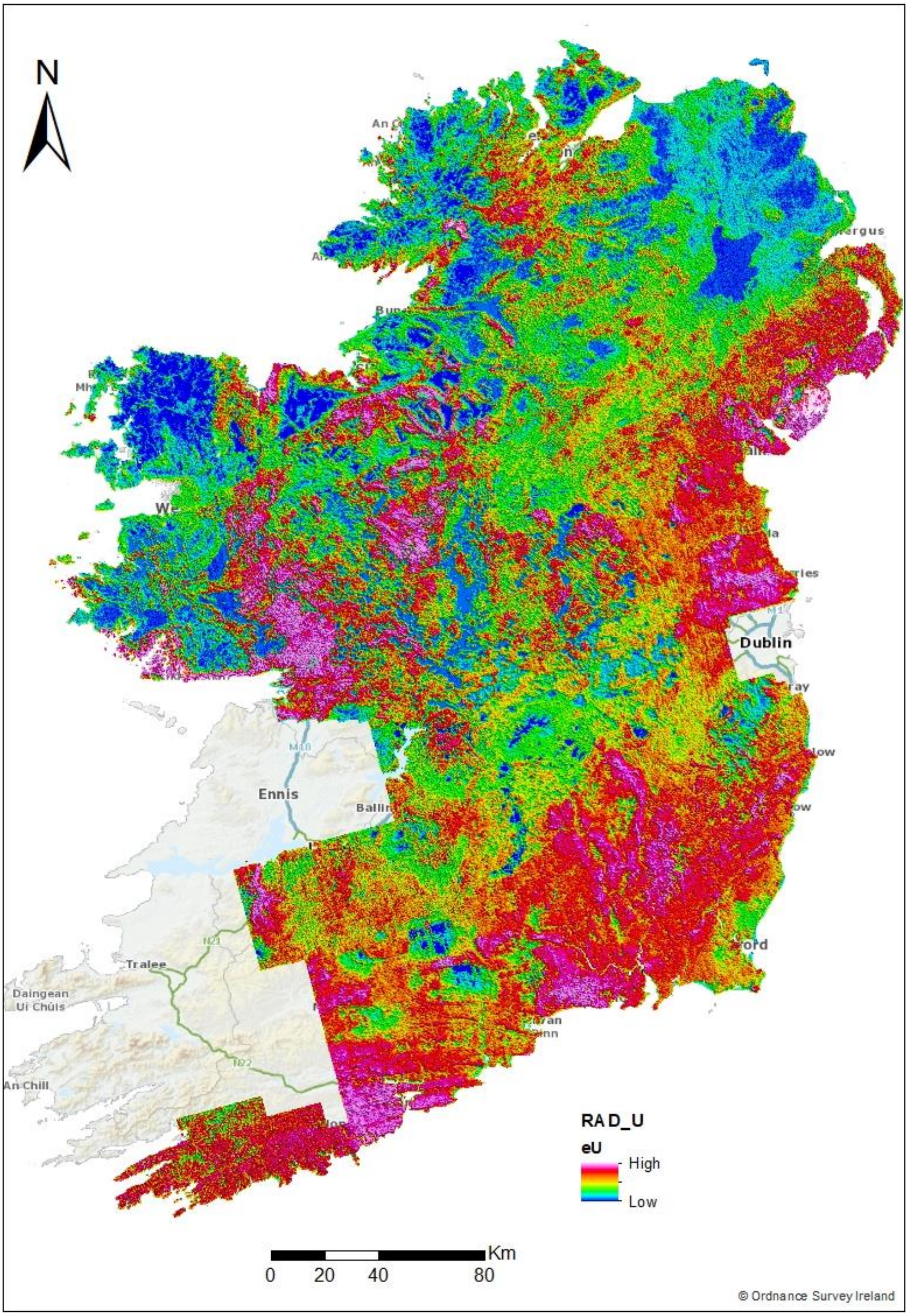

Figure 24: Merged total equivalent Uranium data (eU in ppm) from *Merge2019B*, A8, A9 and A6 blocks. This final merge is referred to as *Merge2022*.

Figure 25: Merged radiometric Ternary map from *Merge2019B*, A8, A9 and A6 blocks. This final merge is referred to as *Merge2022*. Potassium - red, Uranium - blue and Thorium – green.

8.5 Electromagnetic data merging

Overview of four previous and current EM merges

1. *Merge2016*
This includes data from NI, CAV, TB, TNM, A1 and A2 blocks. One of the main complications in merging the electromagnetic data (*Merge2016*) from the various different Tellus survey blocks is that both Time (TEM) and Frequency domain (FEM) data have been collected. Prior to 2016, data have been merged for the different survey phases (or blocks) based on derived conductivities at specified depths for both FEM & TEM datasets. This approach requires inversion of all FEM data producing apparent *conductivities* at certain depths, which can then be merged with conductivity depth transforms of the Time domain data at the same specified depths. However, merging all data from all the survey phases, including those from Northern Ireland (2005-2006), is an extremely time-consuming task. In addition, the inversion of the data results in significant smoothing of the data and a loss of resolution in parts. Therefore, a different approach, using equivalent frequencies, was used to obtain *Merge2016*. This equivalent frequency approach is based on the delay and diffusion times of the TEM data and the diffusion depths of the FEM data. Time gates (delay times) from the TEM data were identified that are equivalent to the 0.9 kHz, 3 kHz, 12 kHz and 25 kHz FEM channels and used for merging. Only two frequencies (3 kHz and 12 kHz) were used because during the first Tellus survey in the western half of Northern Ireland only 2 frequencies were recorded.

These two frequencies (12 and 3 kHz) correspond to time gate 1 and time gate 3 (Table 23) from the TNM dataset, which used the CGG GENESIS system (CGG, 2015). Taking the derived apparent resistivity from the corresponding frequency, or time gate channel, the data were merged for each frequency (12 kHz and 3 kHz). The details of merging processes were given in Hodgson and Ture (2017).

2. *Merge2017*
This includes data from NI, TB, CAV, TNM, A1, A2, A3 and A4. EM data from *Merge2016* (NI, TB, CAV, TNM, A1 and A2) have been merged with A3 and A4 blocks to form a single EM dataset for the entire area surveyed to date as part of the Tellus Programme. The A3 and A4 blocks were designed to include an area of overlap with previous survey blocks so as to help the merge of new data. These new data blocks were compared in the regions of overlap with *Merge2016* and correction factors established. These correction factors were then applied to the older dataset. Details of *Merge2017* are given in Hodgson and Ture (2017). The merged data, *Merge2016*, are in *conductivity* units (mS/m), while the recently acquired A3 and A4 were delivered in resistivity units and in ppm values. Two frequencies 3 and 12 kHz were merged within *Merge2017* and the dataset was released in conductivity units. The difference between *Merge2016* and *Merge2017* is that *Merge2016* was merged conductivity data at specified depths (e.g., 10, 20, 30 m depths) while *Merge2017* is a conductivity merge, not at specified depths but at two frequencies.

3. *Merge2019*
As the Tellus survey progressed from year to year and a number of stakeholders (including Universities) expressed interest in data analysis and depth investigation, GSI decided to provide a four frequency data set. *Merge2019* includes two different data sets: four frequencies were merged for the Republic of Ireland and two frequencies were merged for the island of Ireland. The contractor provided EM data are delivered in resistivity units, while the *Merge2016* and *Merge2017* were publicly released in conductivity units. *Merge2019* has reverted back to resistivity units. The *Merge2019* resistivity data are processed using resistivity values obtained from the HEM inversion method and include NI, TB, CAV, A1, A2, A3, A4 and A5 blocks (TNM is exception as it comprises time domain data). It was decided that the FEM data should be transformed to resistivities for all survey blocks using the same consistent and uniform procedure and same method of levelling. The transformed resistivity values were gridded and checked for leveling errors and

noise. There are only two options to merge the time domain data of the TNM block with the of frequency domain data of all the other blocks. One method is to invert (most easily in 1D) all frequency domain data, and merge the resulting resistivity models with time domain conductivity depth imaging (CDI) model data (provided by contractor CGG) at given depths. Such 1D inversion modelling is extremely time consuming, and furthermore, the CDI model data provided by the contractor (CGG) is not always compatible with 1D inversion results. The other method is the time and frequency equivalence method as described in Sternberg et al., (1988) and Meju (1996). This is formulated by comparing penetration depth of TEM and FEM methods, providing approximate measures of equivalence:

$t = \frac{200}{f}$ (Sternberg et al., 1988) and $t = \frac{256.4}{f}$ (Meju, 1996).

where f is FEM frequency in Hertz (Hz) and t is TEM transient-time in milliseconds (ms).

Table 23 summarises the equivalence between the four Tellus FEM frequencies and TEM transient-time, based on the above equations, and providing the basis for matching FEM frequencies with TEM time gates for the data merge.

4. *Merge2019B*

Merge 2019B includes two different data sets: four frequencies were merged for the Republic of Ireland and two frequencies were merged for the island of Ireland. *Merge2019B* includes *Merge2019* (NI, TB, CAV, A1, A2, A3, A4, A5 and TNM blocks) and A7 and WFD blocks. The procedure for merging *Merge2019B* is the same as for *Merge2019* except for the inclusion of A7 and WFD blocks.

Table 23: Time domain EM (TEM) and frequency domain EM (FEM) equivalence.

TEM time gate number	TEM mid-gate time (µs)	FEM Frequency (Hz)	Equivalence equation used	Equation reference
0	8.68	24510	$(0.2/f)*10^6$	Sternberg et al. (1988)
1	26.04	11962	$(0.256/f)*10^6$	Meju (1996)
3	95.48	3005	$(0.256/f)*10^6$	Meju (1996)
5	243.04	912	$(0.2/f)*10^6$	Sternberg et al. (1988)

5. *Merge2022*

Merge2022 includes three additional data sets: A8, A9 and A6 blocks. Four frequencies were merged for the Republic of Ireland and two frequencies were merged for the island of Ireland. *Merge2022* includes *Merge2019B* (NI, TB, CAV, A1, A2, A3, A4, A5, A7 and TNM blocks) and A8, A9 and A6 blocks. The procedure for merging *Merge2022* is the same as for *Merge2019B* except for the inclusion of A8, A9 and A6 blocks.

8.5.1. Overview of filters used

The company-delivered and levelled In-phase and Quadrature component data for blocks A8, A9 and A6 were transformed into resistivity using the HEM inversion method. Combined Butterworth and directional cosine filters were applied to the new grids so as to remove noise that related to survey flight direction/leveling and unwanted short wavelength noises. The same filter parameters were used for all frequency domain blocks. The filtered grids were compared with *Merge2019B* in the overlap areas and correction factors were established (Table 25). It is to be noted that EM *Merge2022* is merged with respect to the Tellus Border data (unlike the magnetic and radiometric data, which were merged with respect to A6 block, the final block of the merge).

The Butterworth filter was used to apply standard high-pass and low-pass filters. Since the cutoff rolls off over a range of wavenumbers, the outcome does not suffer from the Gibb's oscillation phenomena (Geosoft Technical notes www.geosoft.com). The degree of filter roll-off, centered on the cutoff wavenumber, controls the smoothness of the results along the inflection regions of the strong anomalies. If in these regions oscillation is observed, the user reduces the degree of the filter by one unit and applies the filter again until a satisfactory result is attained. A Butterworth cut-off wavelength of 1600 m (eight times line separation distance) and filter order of 3 to 4 were used for all data.

The directional cosine filter removes directional noise from a grid. The use of a cosine function instead of a straight pass/reject filter overcomes the ringing artefact associated with the discrete Fourier transform. The rejection (or pass) notch can be narrowed or widened by setting the degree of the cosine function so that highly directional features can be isolated. De-corrugation of poorly levelled data is a common application for this filter. A directional cosine cut-off azimuth of 345° (direction of flight) and degree of cosine function of 2 were used.

Every survey line requires a different line number/name to be merged in Geosoft. If two blocks have lines with same number, only one of them is considered in the software when merging them together. The current strategy is to identify line numbers with reference to their block number, for example A1 uses L11001 and A2 uses L21001. However, blocks like TB, CAV, TNM and NI require a naming convention that does not conflict with other blocks. The survey ID (SID) is also included in the merged data to avoid any confusion. Table 24 below indicates the line numbering in the *Merge2022* database.

Table 24: Line naming convention adopted in *Merge2022* TELLUS dataset, with range of line numbers contained in the published dataset.

Block	EM (2F) Line Names		MAG Line Names		RAD Line Names	
	From	To	From	To	From	To
TB	L301000	L302021	B1007	B1946	B1000	B1942
A1	L11001	L11655	S1001	S1660	S1001	S1657
A2	L21008	L21699	R2001	R2694	R2008	R2698
A3	L31002	L31457	L3001	L3458	L3002	L3457
A4	L41003	L41462	L4001	L4468	L4003	L4462
A5	L50001	L50523	L5001	L5525	L5001	L5525
A6	L6007	L6465	L6001	L6465	L6007	L6465
A7	L7001	L7455	L7001	L7459	L7001	L7455
A8	L8001	L8479	L8001	L8479	L8001	L8479
A9	L9001	L9230	L9001	L9230	L9001	L9230
WFD	L311003	L311235	L1001	L1235	L1003	L1235
TNM	P10010	P16110	P10010	P15960	P10010	P15950
CAV	D1003	D1312	D1003	D1312	D1001	D1315
NI	B3	B9331	L10002	L19331	L10002	L19331
Aurum					L3413	L3457

The first step in the merging process of *Merge2022* was comparing grids obtained from *Merge2019B* with those of the A8, A9 and A6 blocks. A summary of the different correction factors applied to EM *Merge2019B*, A8, A9 and A6 to obtain *Merge2022* are summarised in Table 25 below. It is a big challenge to merge the grids where high fly zones are encountered within overlap areas. The high fly areas correlate with very high resistivity values and correction factors computed when including these data proved unreliable in comparison with factors derived when high-fly data were excluded. Therefore, the resistivity model data were clipped to remove data collected at altitudes greater than 150 m, resulting in reliable correction factors and no need for further corrections.

Table 25: Correction factors applied in the creation of merged EM dataset *Merge2022*, based on overlap zones. The high correction factor at overlap between *Merge2021A* and A9 could be due to the large high fly zone percentage in A9 block (see Table 11).

Frequency	**Merge 2019B/A8 => Merge2021A**	**Correction applied**
912 Hz	0.99	0.9*A8
3 kHz	1.1	1.1*A8
12 kHz	1.2	1.2*A8
25 kHz	1.12	1.12*A8
Frequency	**Merge 2021A/A9 => Merge2021B**	**Correction applied**
912 Hz	1.9	1.9*A9
3 kHz	2.1	2.1*A9
12 kHz	1.9	1.9*A9
25 kHz	2.1	2.1*A9
Frequency	**Merge2021B/A6 => Merge2022**	**Correction applied**
912 Hz	1.15	1.15*A6
3 kHz	1.2	1.2*A6
12 kHz	1.3	1.3*A6
25 kHz	1.3	1.3*A6

8.5.2 Levelling of EM data using interactive spectral filter

A filtering procedure was applied to remove levelling artefacts from the merged EM data. Filters were applied to the gridded datasets to help reduce or remove non-geological effects caused by short-wavelength noise along survey lines (Geosoft Technical notes www.geosoft.com). This procedure was performed in Oasis Montaj MAGMAP 2D module using a Fast Fourier Transform (FFT). Combined Butterworth and Directional cosine filters were used. Filter parameters were modified interactively to obtain the best results for the data. Grid preparation consisted of the following steps:

1. Grid trend removal. The trend which is removed is stored in the user area of the grid header and is filtered together with the zero wave number. First order trend removal based on edge points was applied.
2. Expanding the dimensions of a grid by adding dummy areas to the grid edges to produce either a *square* (used for this process) or a rectangular grid. The system uses the Winograd FFT algorithm for dimensions up to 2520 X 2520 cells. Beyond this dimension it switches to a power of 2 FFT method. 10% grid expansion was applied.
3. Replacing all dummies in a grid with interpolated values from the valid parts of the grid. The FFT routines require a completely filled grid resulting in some interpolation of data at the grid edges.

A grid expansion of approximately half the size of the features of interest within the gridded dataset was used. A multistep-expansion method was then used to fill the grid. The multistep expansion method extends the data inside a bounding rectangle within the same range of signal wavelength and amplitude as the real data. After the grid was prepared in the frequency domain, combined Butterworth and Directional cosine filters were applied.

Butterworth filter: applied with cut-off wavelength 1600 m (8 times line spacing distance) and filter order of 3-4 with high pass, so as to create an error grid to isolate short wavelength noise to be removed from the data.

Directional cosine filter: applied with cut-off azimuth of 165°/345° degrees and with degree of cosine function of 2, with pass direction to remove noise related to the survey orientation (flight-line direction) from the data. This filter produces a levelling error grid which can then be removed from the data. This allows high frequency noise along the survey lines to be filtered without minimising the geological signal. An example of the error grid removed from the data is given in Figure 27, with comparisons of the grids before (Figure 26) and after (Figure 28) the noise is removed.

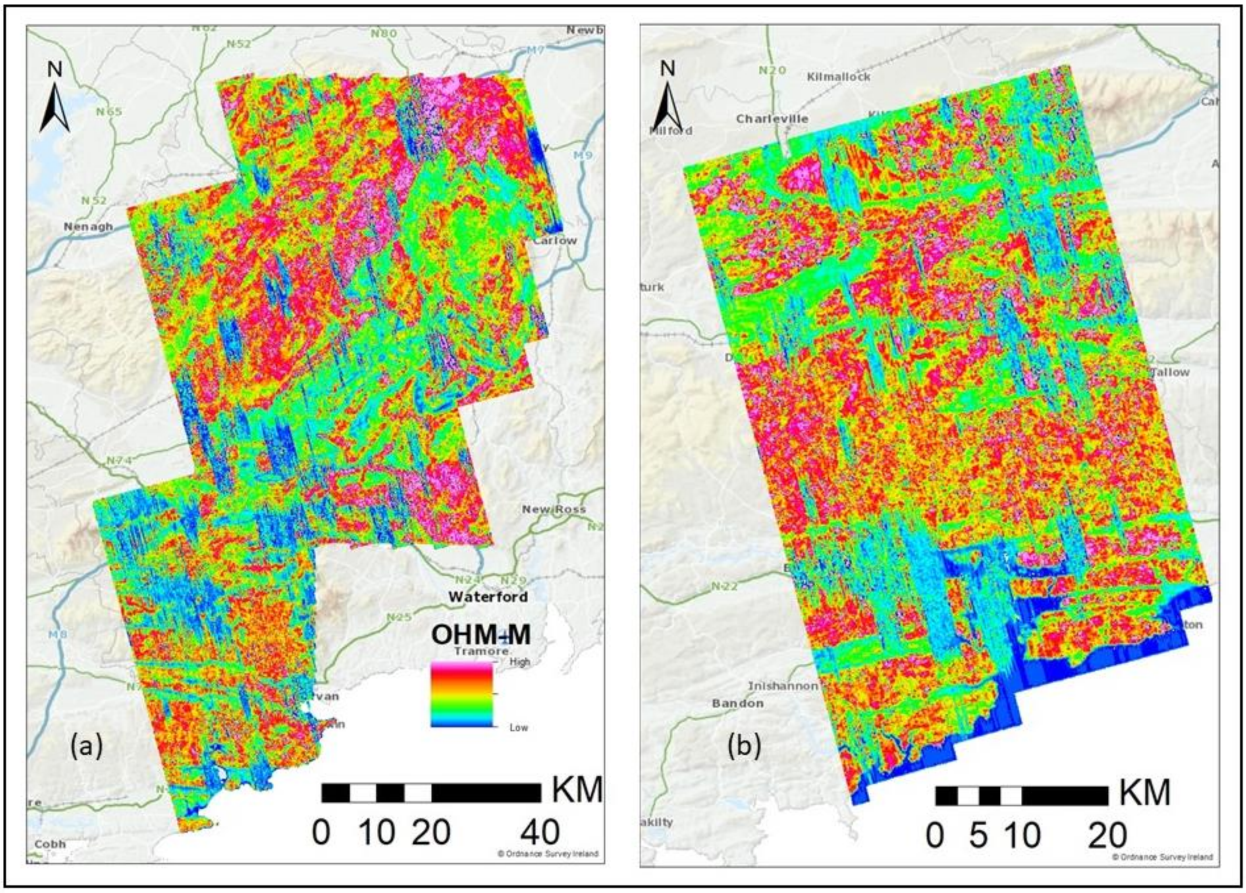

Figure 26: Raw resistivity grids obtained from HEM inversion for A8 (a) and A9 (b) blocks for 3 kHz data. Noise related to survey direction and the effects of high-fly are obvious in the grids.

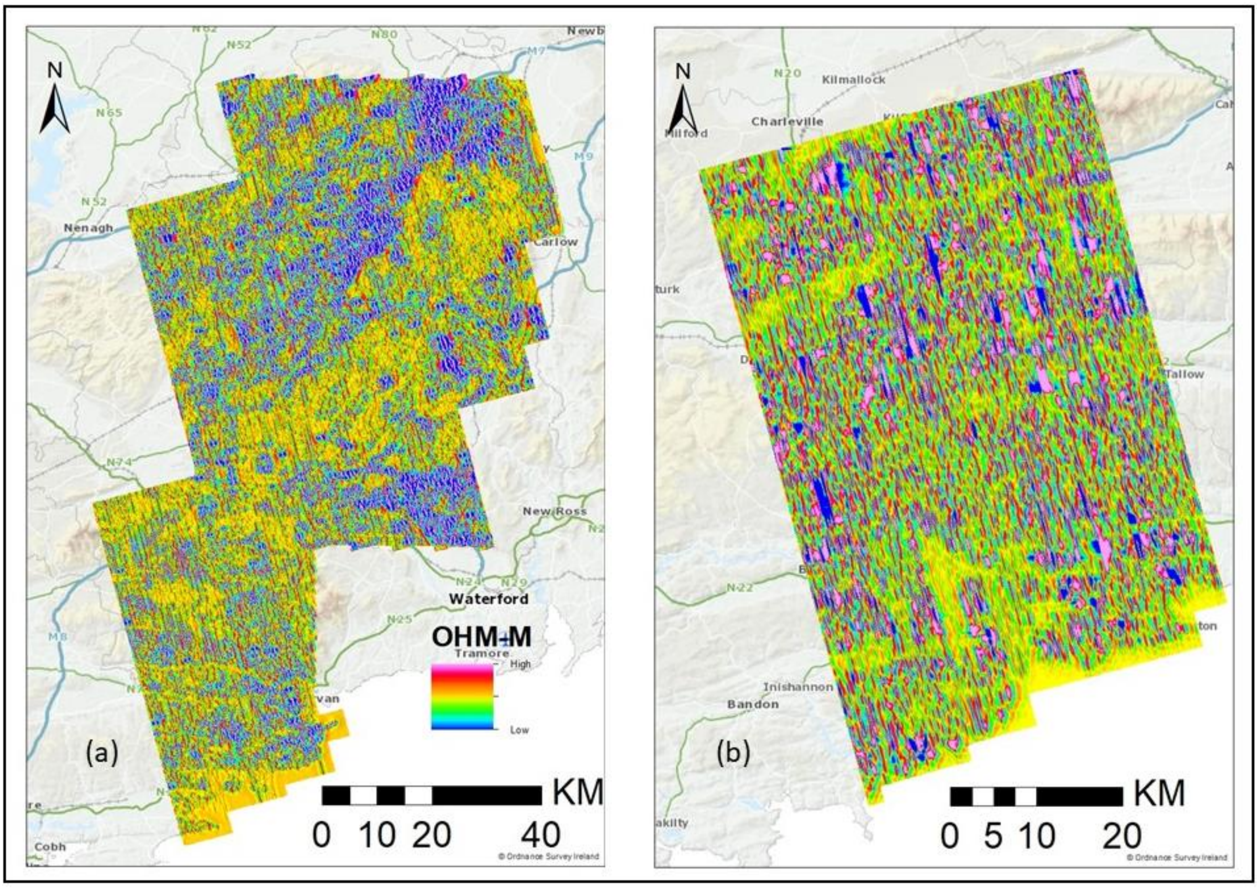

Figure 27: Error grids obtained by combined Butterworth and Directional cosine filters for A8 (a) and A9 (b) blocks for 3 kHz. The error grids are sampled into the database and subtracted from the raw HEM model data (Figure 26) to obtain the levelled resistivity grids given in Figure 28.

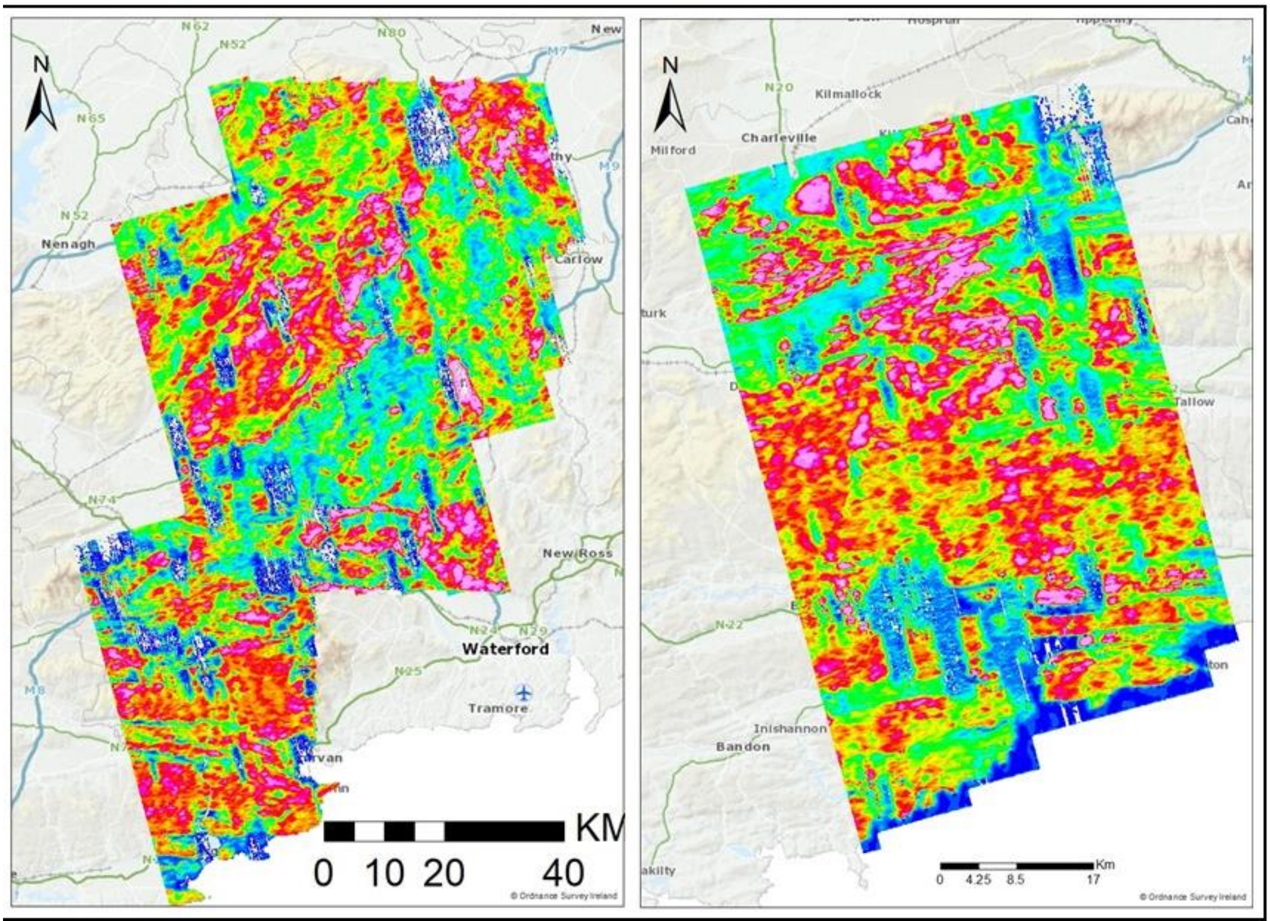

Figure 28: **Levelled resistivity grids for A8 (left) and A9 (right) blocks for 3 kHz obtained by subtracting the error grid (Figure 27) from the original raw HEM model grid (Figure 26).**

8.5.3 Final merged EM grids

The grid of apparent resistivity for the newly created *Merge2022* (TB, NI, TNM, A1, A2, A3, A4, A5, A6, A7, A8, A9 and WFD) was sampled back into the master database. The data are dominated by high conductivity effects over the sea, which can mask (in images) detailed geological information. Because of this, the final merged EM data have been trimmed to the Irish coastline.

Results of the merged apparent resistivity for the four frequencies for Republic of Ireland and two frequencies for the island of Ireland are shown below in Figures 29 – 32 and Figures 33 – 34 respectively, (high altitude areas (>150 m) have been clipped from the data).

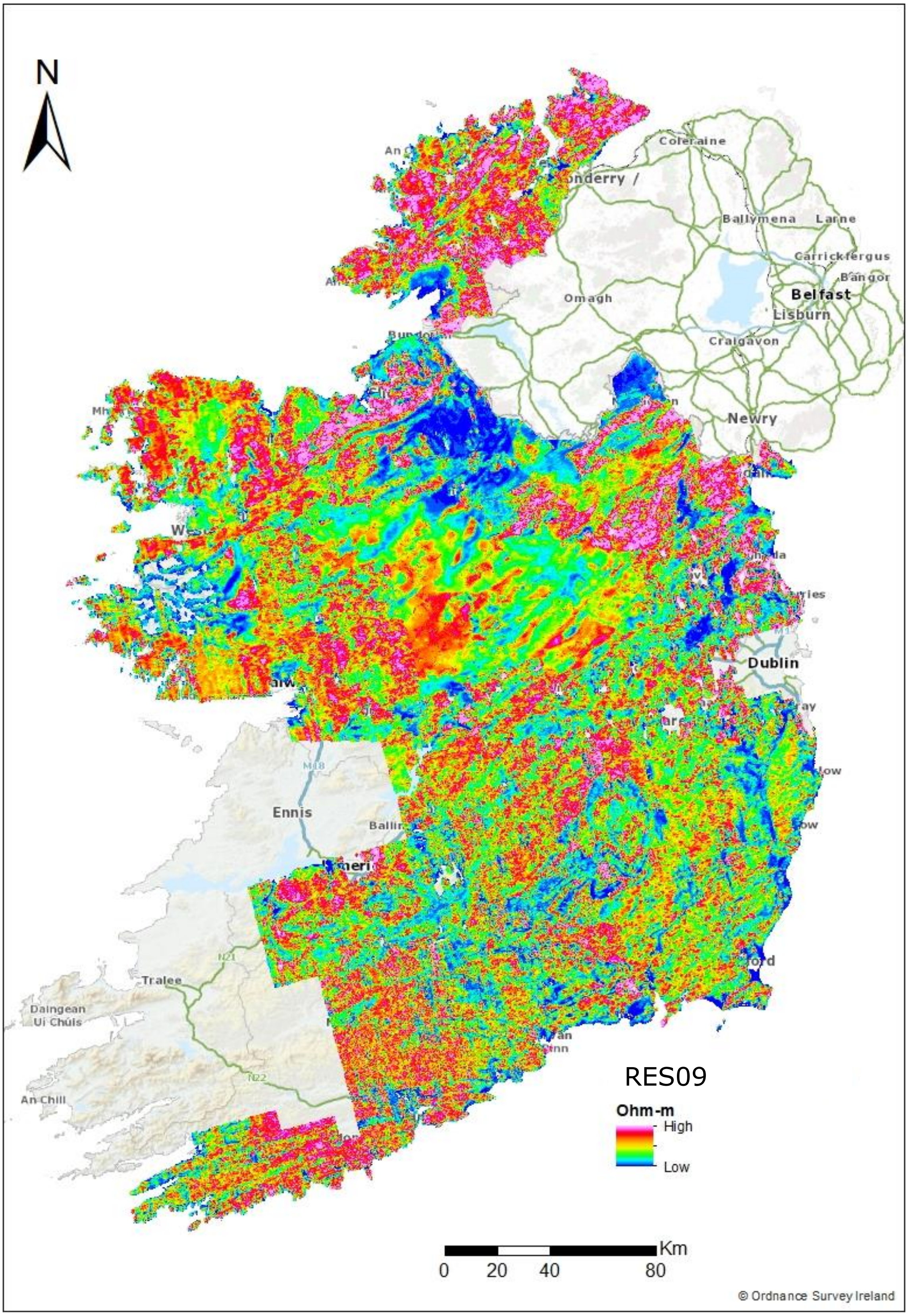

Figure 29: **Four-frequency EM *Merge2022* (NI, TB, CAV, TNM, A1, A2, A3, A4, A5, A7, A8, A9, WFD and A6): merged apparent resistivity for 912 Hz.**

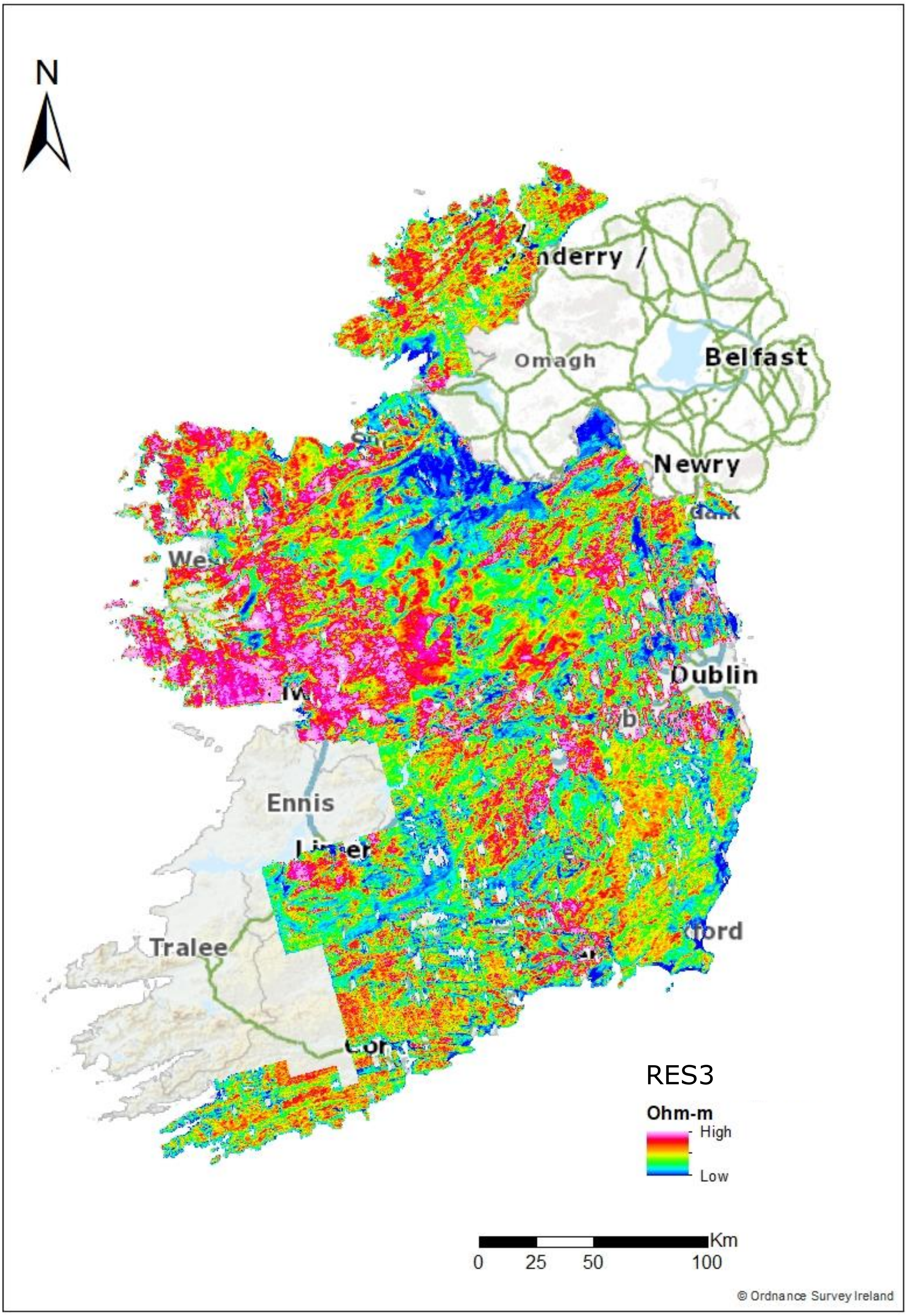

Figure 30: **Four-frequency EM *Merge2022* (TB, CAV, TNM, A1, A2, A3, A4, A5, A7, A8, A9, WFD and A6): merged apparent resistivity for 3 kHz.**

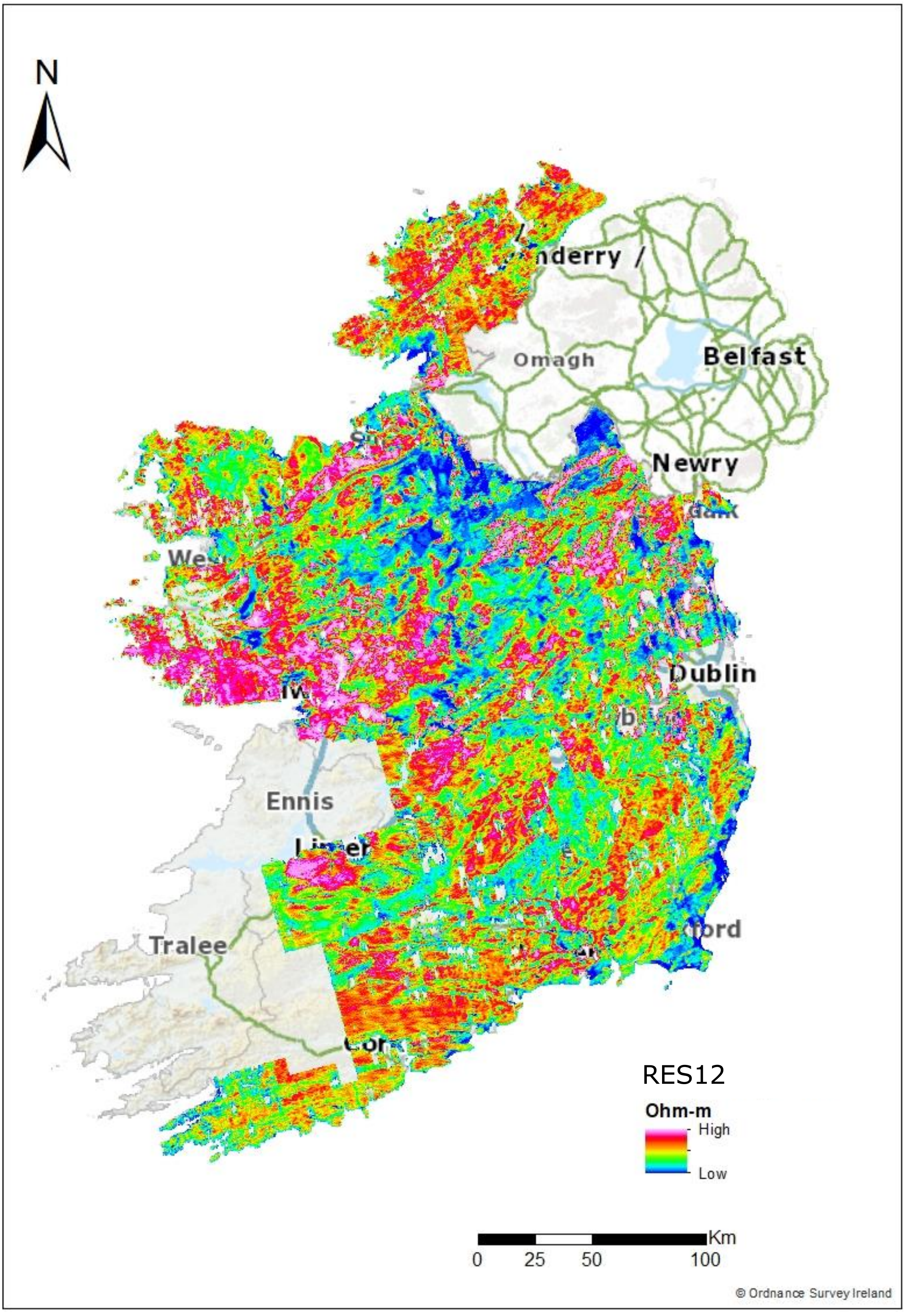

Figure 31: **Four-frequency EM *Merge2022* (TB, CAV, TNM, A1, A2, A3, A4, A5 ,A7, A8, A9, WFD and A6): merged apparent resistivity for 12 kHz.**

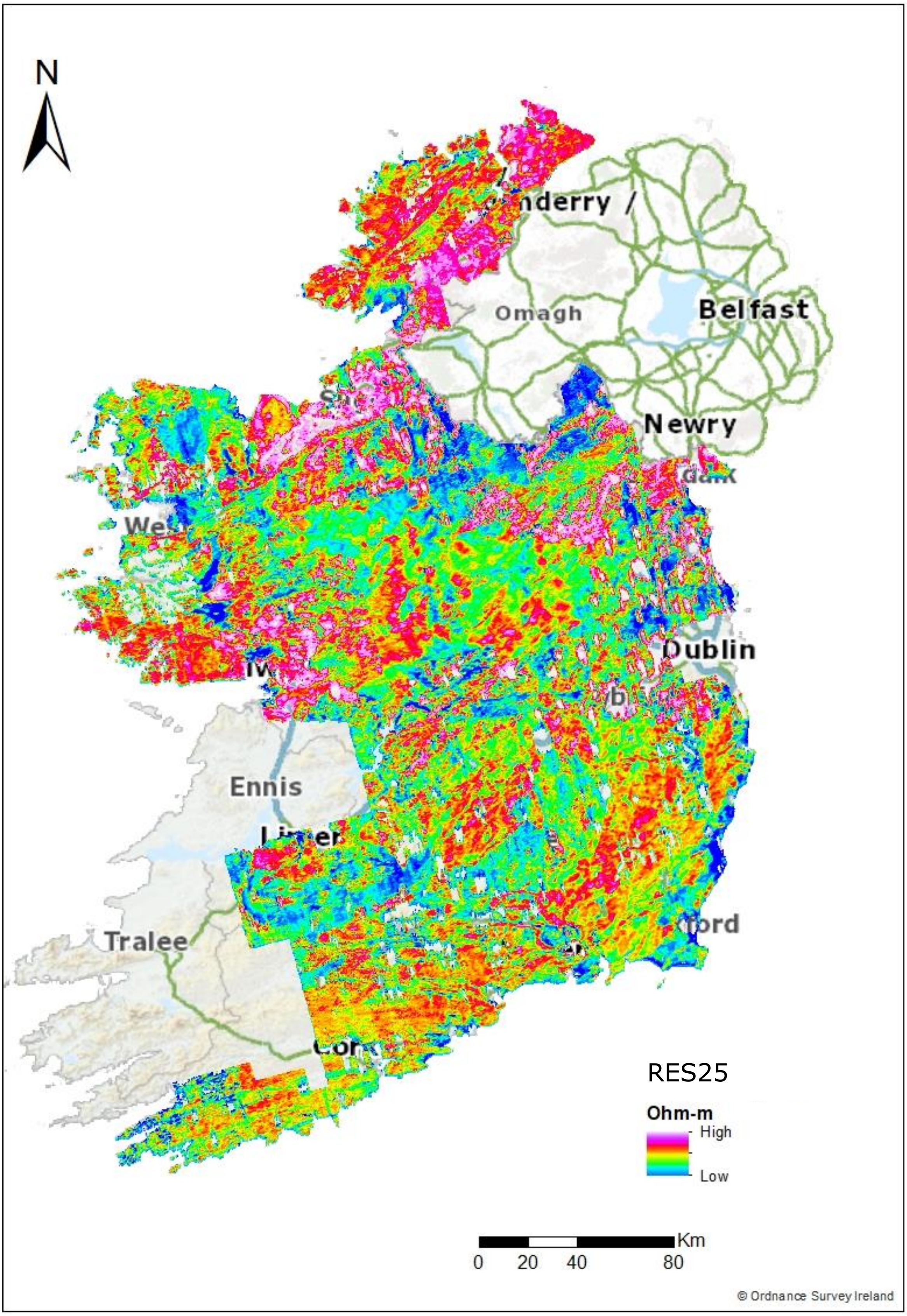

Figure 32: **Four-frequency EM *Merge2022* (TB, CAV, TNM, A1, A2, A3, A4 ,A5, A7, A8, A9, WFD and A6): merged apparent resistivity for 25 kHz.**

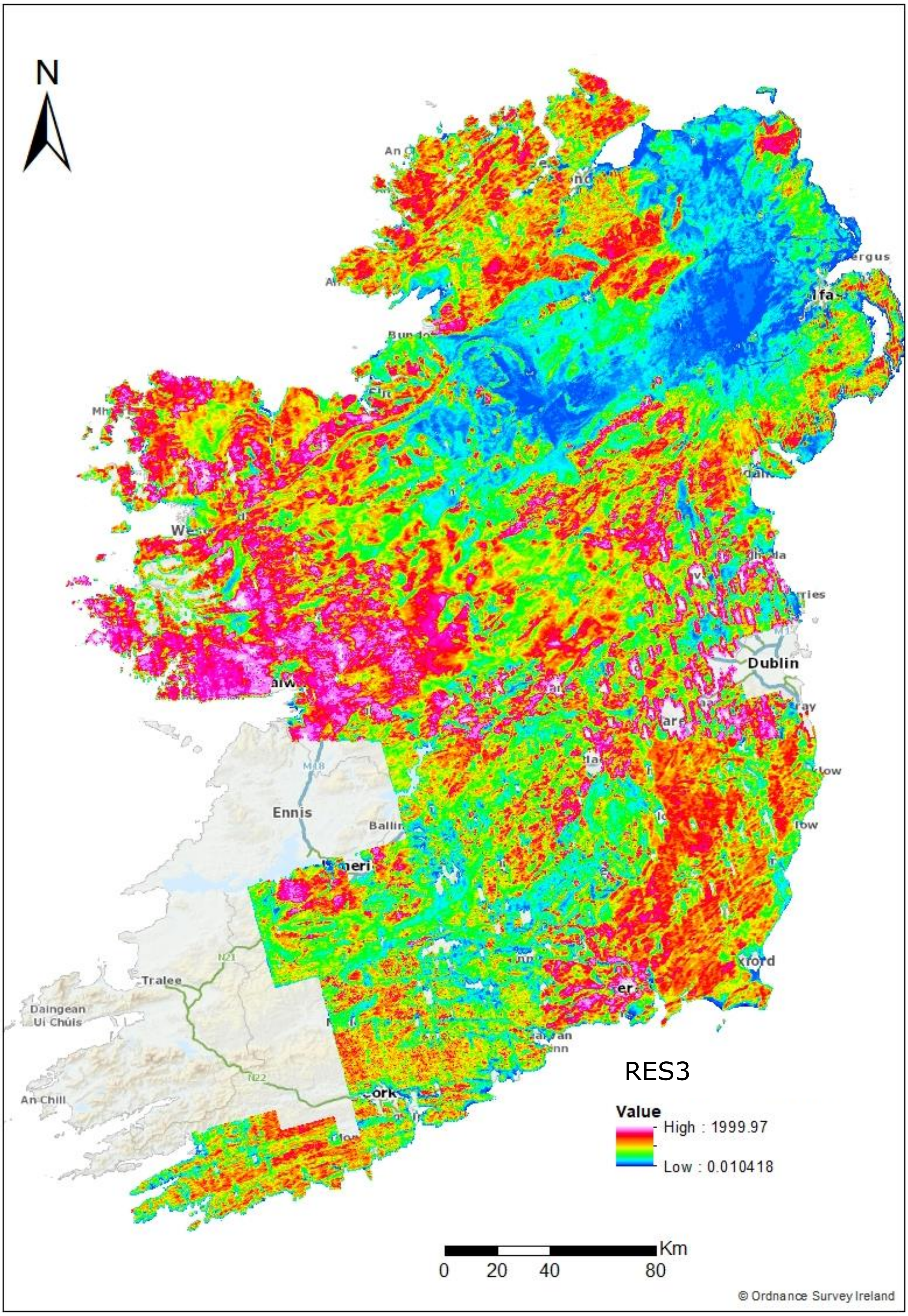

Figure 33: Two-frequency EM *Merge2022* (NI, TB, CAV, TNM, A1, A2, A3, A4, A5, A7, A8, A9, WFD and A6): merged apparent resistivity for 3 kHz.

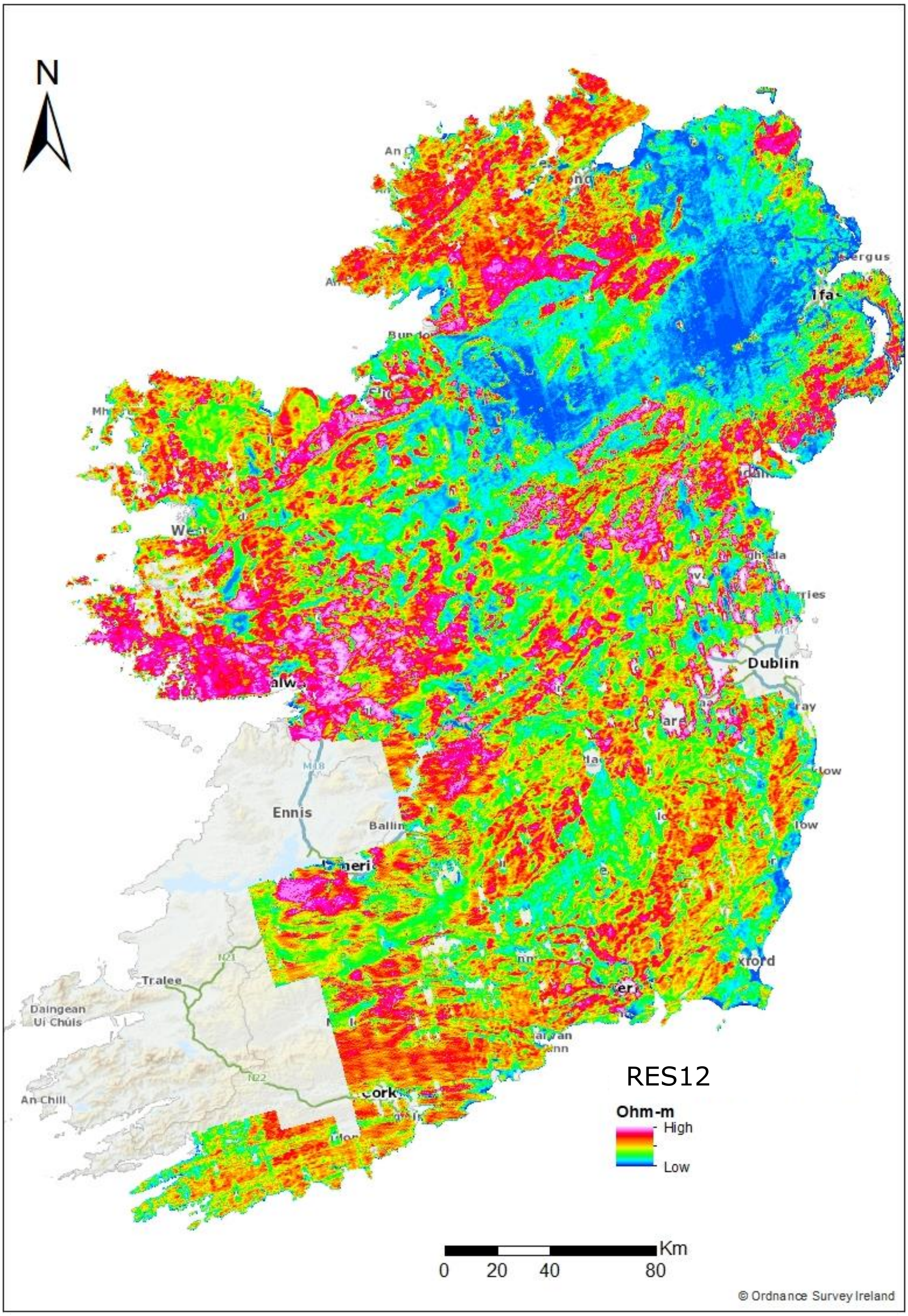

Figure 34: Two-frequency EM *Merge2022* (NI, TB, CAV, TNM, A1, A2, A3, A4, A5, A7, A8, A9, WFD and A6): merged apparent resistivity for 12 kHz.

9. Data Assessment and Consideration

9.1 High Fly Zones

Survey altitude has a major impact on the electromagnetic signals, with increasing altitude attenuating the signal. Increasing altitude also reduces the effective depth of penetration of the system, particularly for FEM data. Although HEM inversion improves the modelling results by effectively nulling the models where high data errors are recorded (i.e., no model solutions can be found), the FEM model data are additionally nulled over high flight altitudes (>150 m) for all blocks except TNM, as investigation of the data recorded over the Bundoran and Waterford test-lines at different survey altitudes has shown model quality and reliability to deteriorate at altitudes greater than 150 m. The reason why TNM block has not been clipped above 150 m altitude is that the TEM system doesn't suffer from high flight-altitude effects when compared to frequency domain systems.

The Tellus Border, TNM, A1, A2, A3, A4, A5, A6, A7, A8, A9, WFD and A6 surveys were issued with a flying permit from the Irish Aviation Authority (IAA) for 60 m flight altitude in non-congested (rural) areas. However, in upland areas, which are affected by aircraft climb and descend rates, along with the presence of numerous wind farms, some areas have been surveyed at higher altitudes. The Tellus North Midlands (TNM) survey was flown at a nominal survey altitude of 90 m (with the EM receiver bird suspended 45m below the aircraft) with a drape system. Numerous enforced high flown zones were often clustered together around urban areas across the region and has resulted in large areas of high fly zones. Figure 36 shows areas where the altitude flown was greater than 150 m and data in these areas should be deemed to be less reliable (particularly FEM data).

Gamma-ray spectrometry data is also sensitive to survey altitude, with a decrease in Gamma-rays sampled with increasing altitude. Although less sensitive than frequency-domain EM systems and with a larger crystal volume used in the A1, A2, A3, A4, A5, A6, A7, A8, A9 and Waterford surveys, data recorded at altitudes greater than 250 m are considered less reliable, even when allowing for altitude corrections made to the radiometric data. Surveys using larger crystals (A1, A2, A3, A4, A5, A6, A7, A8 A9 and Waterford) can have good data at altitudes greater than 250 m but only if measured counts are reasonable high, and therefore should be reviewed on a line-by-line basis. Any data from altitudes greater than 450 m should be removed as potentially erroneous.

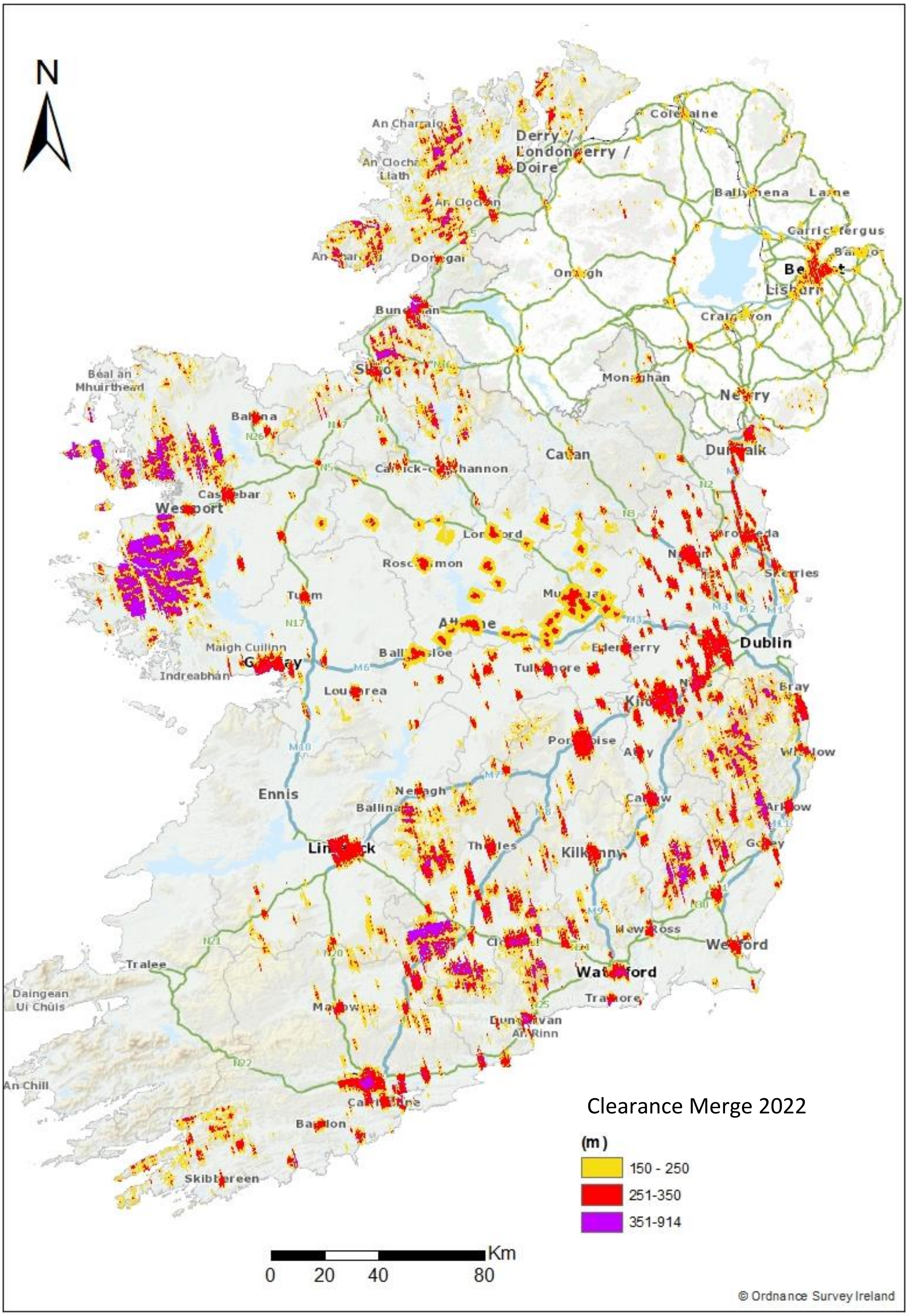

Figure 35: **Survey flight altitudes greater than 150 m above ground level shown in yellow, greater than 250 m shown in red and greater than 350 m shown in purple.**

As can be seen from Figure 35, significant high fly zones (> 150 m) are present across the entire surveyed region. High-fly zones include urban areas with populations greater than 2,500 people; areas along the M1, M6 and M7 motorway corridors in counties Dublin, Meath, Westmeath, Kildare and Limerick; areas over sensitive livestock and stud farms; areas with requests for high-fly from the public; and hilly terrain particularly in the northwest, west and southeast of the area.

9.2 Magnetic Noise

Magnetic data were measured using Geometrics G-822A caesium vapour magnetometers, which have a sensitivity of 0.005nT. Figures of Merit (FOM), derived from magnetic compensation tests during the A1, A2, WFD, A3, A4, TB and TNM surveys, showed values in the range of 0.4 nT to 1.28 nT. For A5 and A6 blocks two sets of compensations (with FOMs) were used: 1.25 nT for flights 001-0069 and 1.71 nT for flights 0070-0082. For the A7 block, the FOM used for all flights was 1.14 nT. For A8 and A9 the FOM used was 1.07 nT.

Cultural interference is the main source of noise affecting the data. Cultural interference from anthropogenic sources, such as houses, farm buildings, roads, power lines, etc., creates spikes throughout the data. Data from Tellus Border, Cavan, Tellus North Midlands, A1, A2, A3, A4, A5, A6, A7, A8, A9 and Waterford datasets were not subjected to numerical de-culturing. However, a number of well-developed smoothing procedures are available. The upward continuation method is widely used and it does not produce mathematical artefacts. This method could be used to minimize high frequency cultural noise in the magnetic data.

Diurnal and IGRF corrections have been made to all datasets. All data have been corrected to the most recent model of the IGRF. The largest corrections due to IGRF are found in the north of the survey areas because of increased latitudes.

9.3 Radiometric Noise

To assist in the assessment of the radiometric data, a 6 km test line was flown throughout the duration of Tellus Border survey and at the beginning and end of all the Tellus survey blocks. The NI, TB, CAV, TNM, A1, A2, A3, A4, A5, A6 and Waterford surveys used the Bundoran test line. As the airborne survey progressed towards the south, a new test line was established near Waterford city. From A7 survey block onwards, the Waterford test line has been used. The test line was flown at different nominal altitudes and crossed from sea to land. The test line data, once re-sampled, allows direct comparisons at the same locations to be made over the duration of the survey, giving insight into the sensitivity of the system and any environmental impacts. Total count data along the Bundoran test line during the A7 survey and also from previous phases show that readings vary by factors of +/-5% between individual flights. This would therefore indicate that measured values vary by up to 5% from the mean.

Rainfall data were taken from the Finner Meteorological Station in Co. Donegal, which lies approximately 7 km to the NW of the test line to assist in the assessment of seasonal effects. As expected a negative relationship exists between total counts and increasing rainfall, whereby for every ~1 mm increase in rainfall, total count values decrease by about 0.8%. Rainfall data were taken for each day of the flight, as well as over a 3-day average and 14-day average. Taking rainfall only on the day of each flight may have incurred errors as the measurement was for the entire day and flights may have occurred before any measured rainfall for that day. The 3 and 14-day averages may indicate the degree of saturation of the ground. Recent studies have investigated how both soil and bedrock type, together with the degree of saturation of the ground, can influence the attenuation of gamma rays (Beamish, 2013 and Beckett, 2008).

9.4 Electromagnetic noise

Both frequency-domain and time-domain electromagnetic data are particularly prone to electromagnetic field interference from power lines, buildings and electric fences, which can create sources of noise that cannot easily be resolved. The amplitudes of the measured coupling ratios, or corresponding time gate channels, decrease over areas of high resistivity/low conductivity. Because of this, the signal-to-noise ratio is reduced in highly resistive areas sometimes making it impossible to distinguish the true (geological) signal. In resistive zones, levelling of the data also becomes more difficult and can result in small amplitude undulations. This is particularly the case for the low frequencies within FEM systems, as they are most susceptible to highly resistive zones (Hautaniemi *et al.,* 2005). Time domain data seems less affected by cultural noise affects and is generally able to penetrate deeper into the earth (depending on the time windows used).

Survey altitude has a major impact on the electromagnetic signals with increasing altitude attenuating the signal. Increasing altitude also reduces the effective depth penetration of the system, particularly for FEM data. It is, therefore, recommended that FEM data collected at survey altitudes exceeding 150 m should be considered with care. TEM data are less affected and should be reviewed on a case-by-case basis. Typically, the measured FEM data can be inverted to consistent depths of around 60 m bgl, while the TEM data can extend to depths of 200 m. Therefore, the merging of resistivity data from the two systems can only be reasonably derived for the upper 60 m depth.

Full details of the electromagnetic processing and a review of the inversion procedure can be found in Beamish (2013), Hodgson and Ture (2013), CGG (2015), SGL (2015, 2016), and Ture and Hodgson (2017, 2019).

9.5 Data filtering

There are many different approaches to data filtering; however, it has been decided that Geological Survey Ireland will provide data for public use with the minimum processing and filtering. This will allow the individual user to perform their own processing and filtering of the data to their own requirements and specifications. Therefore, no additional filtering of the magnetic and radiometric data has been carried out. The EM processing has been discussed in section 8.5 above and the applied filters are minimal and don't create artefacts. The delivered data consist of the contractor supplied final data and merged data, with corrections applied only to allow seamless merging of different datasets. Additional filtering may be required, i.e., upward continuation of magnetic data to remove cultural interference, etc. The merged magnetic images are pole-reduced and upward continued 250 m distance to get cleaner data (particularly, first vertical derivative and tilt derivative), and additional filtering was not applied.

10. Data Delivery

10.1 Overview & Delivered Data

Standard processing was performed on all three datasets (1, Magnetics; 2, Radiometrics; and 3, EM) by the contractor and are discussed in detail in Beamish *et al*., 2006 and reviewed by Hodgson and Ture (2013) for Tellus Border and Cavan-Monaghan data, and by CGG (2015) for the Tellus North Midlands data and by SGL (2015, 2016, 2017, 2018-2019) for the A1, A2 and WFD blocks and by SGL (2017a and 2017b) for A3 and A4 blocks, SGL (2018-2019a) for A5 and A6 blocks, SGL (2019b) for A7 block and SGL (2021) for A8 block. The contractor's supplied data is in ASCII.xyz and Geosoft grid formats. Additional processing applied to the EM data was also undertaken by GSI and has been discussed in Sections 7 and 8.

The merge of the new A8, A9 and A6 data with the previous Merge2019B datasets has been outlined in Section 8. As the number of merged blocks become larger, the data file increases in size making data downloads difficult. Hence, only critical data channels, as shown in Tables 26-29, are now included for data download. Contractor supplied data for each survey phase are also available for download or upon request from www.gsi.ie/tellus.

Table 26: *Merge2022*: A1, A2, A3, A4, A5, A6, A7, A8, A9, TNM, TB, CAV, NI and WFD magnetic merged data channels.

No	***Name***	***Units***	***Description***
1	X_ITM	m	X coordinate, Irish Transverse Mercator
2	Y_ITM	m	Y coordinate, Irish Transverse Mercator
3	DATE	YYYYMMDD	Date (year, month, day)
4	RALT	m	Radar altitude (height above ground)
5	SID	-	Survey ID (A1, A2, A3, A4, A5, A6, A7, A8, A9, TB, CAV, TNM, NI and WFD)
6	MAG_MERGE_2022	nT	Magnetic Anomaly (IGRF & Diurnal corrected, Levelled)

Table 27: *Merge2022*: A1, A2, A3, A4, A5, A6, A7, A8, A9, TNM, TB, CAV, NI and WFD radiometric merged data channels.

No	***Name***	***Units***	***Description***
1	X_ITM	m	X coordinate, Irish Transverse Mercator
2	Y_ITM	m	Y coordinate, Irish Transverse Mercator
3	DATE	YYYYMMDD	Date (year, month, day)
4	CLEARANCE	m	Altimeter height above ground
5	SID	-	Survey ID (A1, A2, A3, A4, A5, A6, A7, A8, A9, TB, CAV, TNM, NI and WFD)
6	TC_MERGE_2022	cps	Merged Corrected Total Count
7	TH_MERGE_2022	ppm	Merged Corrected Thorium Concentration
8	K_MERGE_2022	%	Merged Corrected Potassium Concentration
9	U_MERGE_2022	ppm	Merged Corrected Uranium Concentration

Table 28. ***Merge2022*****: A1, A2, A3, A4, A5, A6, A7, A8, A9, TNM, TB, CAV, NI and WFD EM_2F Resistivity data channels.**

Number	***Name***	***Units***	***Description***
1	X_ITM	m	X coordinate, Irish Transverse Mercator
2	Y_ITM	m	Y coordinate, Irish Transverse Mercator
3	DATE	YYYYMMDD	Date (year, month, day)
5	CLEARANCE	m	Altimeter height, height above ground
4	SID	-	Survey ID (NI, TB, CAV, TNM, A1, A2, A3, A4, A5, A6, A7, A8, A9, and WFD)
6	RES3_MERGE_2022	Ohm-m	Apparent Resistivity derived from HEM inversion of 3 kHz data & TEM equivalent data
7	RES12_MERGE_2022	Ohm-m	Apparent Resistivity derived from HEM inversion of 12 kHz data & TEM equivalent data

Table 29. ***Merge2022*****: A1, A2, A3, A4, A5, A6, A7, A8, A9, TNM, TB, CAV and WFD, EM_4F Resistivity data channels.**

1	X_ITM	m	X coordinate, Irish Transverse Mercator
2	Y_ITM	m	Y coordinate, Irish Transverse Mercator
3	DATE	YYYYMMDD	Date (year, month, day)
4	CLEARANCE	m	Altimeter height, height above ground
5	SID	-	Survey ID (TB, CAV, TNM, WFD, A1, A2, A3, A4, A5, A7, A8, A9)
6	RES09_MERGE_2022	Ohm-m	Apparent Resistivity derived from HEM inversion of 912 Hz data & TEM equivalent data
7	RES3_MERGE_2022	Ohm-m	Apparent Resistivity derived from HEM inversion of 3 kHz data & TEM equivalent data
8	RES12_MERGE_2022	Ohm-m	Apparent Resistivity derived from HEM inversion of 12 kHz data & TEM equivalent data
9	RES25_MERGE_2022	Ohm-m	Apparent Resistivity derived from HEM inversion of 25 kHz data & TEM equivalent data

All data were processed and exported using the Oasis Montaj Geosoft programme and are available in .xyz ascii format.

It is the policy of Geological Survey Ireland that all data are free. Data can be downloaded from the project website www.gsi.ie/tellus.

References

IAEA, 2003. Guidelines for radioelement mapping using gamma ray spectrometry data. International Atomic Energy Agency, Technical Report Series, No. 1363. http://www-pub.iaea.org/mtcd/publications/pdf/te_1363_web.pdf

Beamish, D., 2013. Gamma ray attenuation in the soils of Northern Ireland, with special reference to peat. Journal of Environmental Radioactivity, 115, 13-27.

Beamish, D., Cuss, R.J., Lahti, M., Scheib, C. and Tartaras, E., 2006. The Tellus Airborne Geophysical Survey of Northern Ireland: Final Processing Report. British Geological Survey Technical Report IR/06/136. A report prepared for DETI, Belfast. http://nora.nerc.ac.uk/7427/1/IR06136.pdf

Beckett, K., 2008. Multispectral processing of high-resolution radiometric data for soil mapping. Near Surface Geophysics, 6, 281-287.

CGG, 2015. Logistics and Processing Report: GENESIS Airborne Electromagnetic, Magnetic and Radiometrics Geophysical Survey, Project AIRJ2621.

Geosoft Technical notes www.geosoft.com),Microleveling using FFT Decorrugation and Interactive Filtering Method in MAGMAP.

Geosoft Technical notes (www.geosoft.com), Applying filters and Inverse FFT in- MAGMAP

Grasty, R.L. and Minty, B.R.S., 1995. A guide to the technical specifications for airborne gamma-ray surveys. Australian Geological Survey Organisation, Record, 1995/20.

Hautaniemi, H., Kurimo, M., Multala, J., Leväniemi, H. and Vironmäki, J., 2005. The 'three in one' aerogeophysical concept of GTK in 2004. In: Airo, M-L. (ed.) Aerogeophysics in Finland 1972-2004: Methods, System Characteristics and Applications. Geological Survey of Finland, Special Paper 39, 21-74.

Helicopter Electromagnetic data processing, Analysis and Presentation system for Oasis montaj (V6.2) tutorial and user guide

Hodgson, J.A. and Ture M.D., 2013. Tellus Border Airborne Geophysics Data Processing Report Version 2. Geological Survey of Ireland / Geological Survey of Northern Ireland joint report. (http://www.tellusborder.eu/NR/rdonlyres/7E6942A1-90BA-4E57-B5D0-1AC27A041ED6/0/TellusBorder_Processing_Report_Version_1_FINAL_Appendix.pdf

Hodgson, J.A. and Ture M.D., 2015. Processing and data merging report of Tellus Airborne geophysical datasets, 2012-2015. Geological Survey of Ireland Report. (http://www.tellus.ie/Data/TNM_Geophysics-Processing-Merging_report_Sep2015.pdf.)

Hodgson J.A. &. Ture M.D., 2017. Tellus A2 Airborne Geophysical Technical Report (Operations, Logistics and Data Merging) (Galway area). Geological Survey of Ireland Report. (http://www.tellus.ie/about/publications/Geophysical technical and interpretation reports)

Kurimo, M., 2006. High Resolution aerogeophysical survey, Ireland. Internal report for the Geological Survey of Ireland.

Meju, M.A., 1996. Joint inversion of TEM and distorted MT sounding: Some effective practical considerations. Geophysics, Vol. 61, No1, pp56-65

SGL, 2015. Technical report: Fixed-Wing High-Resolution Aeromagnetic, Gamma-ray Spectrometry and Frequency-Domain Electromagnetic survey, Tellus A1 Block, Republic of Ireland.

SGL, 2016. Technical report: Fixed-Wing High-Resolution Aeromagnetic, Gamma-ray Spectrometry and Frequency-Domain Electromagnetic survey, Tellus A2 Block, Republic of Ireland.

SGL, 2017a (TR-849A3-2017-000). Technical report: Fixed-Wing High-Resolution Aeromagnetic, Gamma-ray Spectrometry and Frequency-Domain Electromagnetic survey, Tellus A3 Block, Republic of Ireland.

SGL, 2017b (TR-849A4-2017-000). Technical report: Fixed-Wing High-Resolution Aeromagnetic, Gamma-ray Spectrometry and Frequency-Domain Electromagnetic survey, Tellus A4 Block, Republic of Ireland.

SGL, 2019a (TR-861A6-2019-000). Technical report: Fixed-Wing High-Resolution Aeromagnetic, Gamma-ray Spectrometry and Frequency-Domain Electromagnetic survey, Tellus A6 Block, Republic of Ireland.

SGL, 2019b (TR-861A7-2019-003). Technical report: Fixed-Wing High-Resolution Aeromagnetic, Gamma-ray Spectrometry and Frequency-Domain Electromagnetic survey, Tellus A7 Block, Republic of Ireland.

SGL, 2021 (TR-888A8-2021-000). Technical report: Fixed-Wing High-Resolution Aeromagnetic, Gamma-ray Spectrometry and Frequency-Domain Electromagnetic survey, Tellus A8 Block, Republic of Ireland.

Sternberg, B.K., Washburn, J.C. and Pellerin, L., 1988. Correction for static shift in Magnetotellurics using transient electromagnetic sounding. Geophysics Vol.53, no11, pp1459-1468.

Ture M.D. and Hodgson J.A., 2015. Processing and merging time and frequency domain electromagnetic data from the Tellus Airborne geophysical surveys, 2011-2015. Geological Survey of Ireland Report. (http://www.tellus.ie/Data/EM_Merging-Report_TNM_TBCAV_Dec2015.pdf.)